Supporting Information

Highly Efficient Synthesis of *p*-Benzoquinones Catalyzed by Robust Two-Dimensional POM-based Coordination Polymers

Shenzhen Chang, Yanhong Chen, Haiyan An, Qingshan Zhu, Huiyun Luo, Tieqi Xu*

School of Chemical Engineering, Dalian University of Technology, Dalian 116023, People's Republic of China

CONTENTS:

---

*Corresponding author. Tel: +86-411-84657675. E-mail address: anhy@dlut.edu.cn.

I. Supplementary Experimental Section

Materials

All the other reagents were the best available reagent grade without further purification. $H_3PW_{12}O_{40}\cdot xH_2O$, $K_4PW_{11}VO_{40}\cdot xH_2O$, $H_3PMo_{12}O_{40}\cdot xH_2O$, and $((N(C_3H_9)_4)_3PMo_{12}O_{40}$ were synthesized according to the literature,[S1-S5] and confirmed by means of infrared spectroscopy (IR) (Figure S22). The 4-(1H-tetrazol-5-yl)pyridine used in the synthesis process was synthesized according to the literature, and the details are as follows.[S6,S7]

Syntheses of 4-(1H-tetrazol-5-yl)pyridine

Magnetically stirred mixtures of the 4-cyanopyridine (10.41g, 0.1 mol), NH_4Cl (6.9 g, 0.13 mol) and NaN_3 (8.45 g, 0.13 mol) in anhyd DMF (60 mL) were heated to 140 °C for 48 h. (*Note: Sodium azide is explosive*) The cooled mixtures were poured into H_2O (300 mL) and acidified to pH ~ 2 with concentrated hydrochloric acid. After 12 h at 4 °C, the suspension was filtrated and washed with H_2O, H_2O/EtOH (1/1) and H_2O and dried. Recrystallisation from EtOH or propan-2-ol gave analytically pure products. IR (KBr pellet, cm^{-1}, Figure S22): 3438(w), 3099(m), 3037(w), 2969(w), 2529(s), 2111(m), 2025(m), 1631(s), 1629(s), 1440(s), 1388(m), 1354(w), 1292(w), 1251(w), 1200(w), 1186(w),1145(w), 1120(w), 1095(m), 1042(s), 1020(m), 990(m), 870(w), 847(s), 750(s), 714(w), 572(m), 460(s).

Instrumentation and Sample Characterization

Elemental analyses (H, C and N) were performed on a Perkin-Elmer 2400 CHN elemental analyzer; IR spectra were recorded in the range 4000-400 cm^{-1} on a Nexus Euro FT/IR Spectrophotometer using KBr pellets. The powder X-ray diffraction (PXRD) patterns of the as-prepared products were carried out by using Rigaku SmartLab X-ray diffractometer with Cu-Kα radiation (λ = 0.154 nm) and 2θ transforming from 5 to 50°. The X-ray single crystal diffraction of the as-prepared products were collected by Bruker D8 Venture single crystal diffractometer with Mo-Kα radiation. Diffuse reflectivity spectra were collected on a finely ground sample with

a Cary 500 spectrophotometer equipped with a 110 mm diameter integrating sphere, which were measured from 200 to 800 nm. Liquid UV-vis spectrum was measured from 250 to 450 nm on Techcomp UV1000 spectrophotometer. The products in catalytic experiments were determined by gas chromatography with SE-54 capillary column (Techcomp GC 7900II) and gas chromatography-mass spectroscopy (Trace ISQ). The EDS were determined using a JSM-7610F Plus scanning electron microscope at an accelerating voltage of 10 kV. Powder samples were weighed into 4 mm i.d. quartz tubes for the Electron paramagnetic resonance (EPR) spectral measurements. EPR spectra were obtained at ambient temperature (300 K) as first derivatives of the microwave (9.42 GHz) absorption with a Bruker Elesys equipped with X-band EPR spectrometer. The calculation formula of *g*-value is as follows: $g = h\nu/\beta H$ (*h*: planck constant; *v*: microwave frequency; β: Bohr magneton; *H*: magnetic field intensity). X-ray photoelectron spectroscopy (XPS) analyses were performed on a VG Escalab MK-II spectrometer with an Al Ka (1486.5 eV) achromatic X-ray source. Specific surface areas and porosity were determined by measuring the N_2 adsorption−desorption isotherms obtained at 77 K with an Autosorb-IQ2 instrument. The surface area was calculated according to the Brunauer–Emmett–Teller (BET) theory in the range of P/P_0 0–1.0. The pore sizes were calculated using the density functional theory (DFT) method. Before the measurements, the products were outgassed at 150 °C for 24 h under vacuum to ensure the complete removal of any previously adsorbed material.

X-Ray crystallography

The crystal data of **1**-**4** were collected at 150(2) or 300(2) K with graphite monochromatic Mo Kα radiation (λ = 0.71073 Å). The crystal structure was solved and refined by full matrix least-squares methods against F^2 by using SHELXTL-2018 programs.[S8,S9] All non-hydrogen atoms were refined with anisotropic temperature parameters. All hydrogen atoms associated with C and N atoms were placed in geometrically idealized positions using a riding model. Crystallographic data, structure refinements and CCDC reference numbers for **1**−**4** are listed in Tables S3-S7.

II. Supplementary Structure Figures

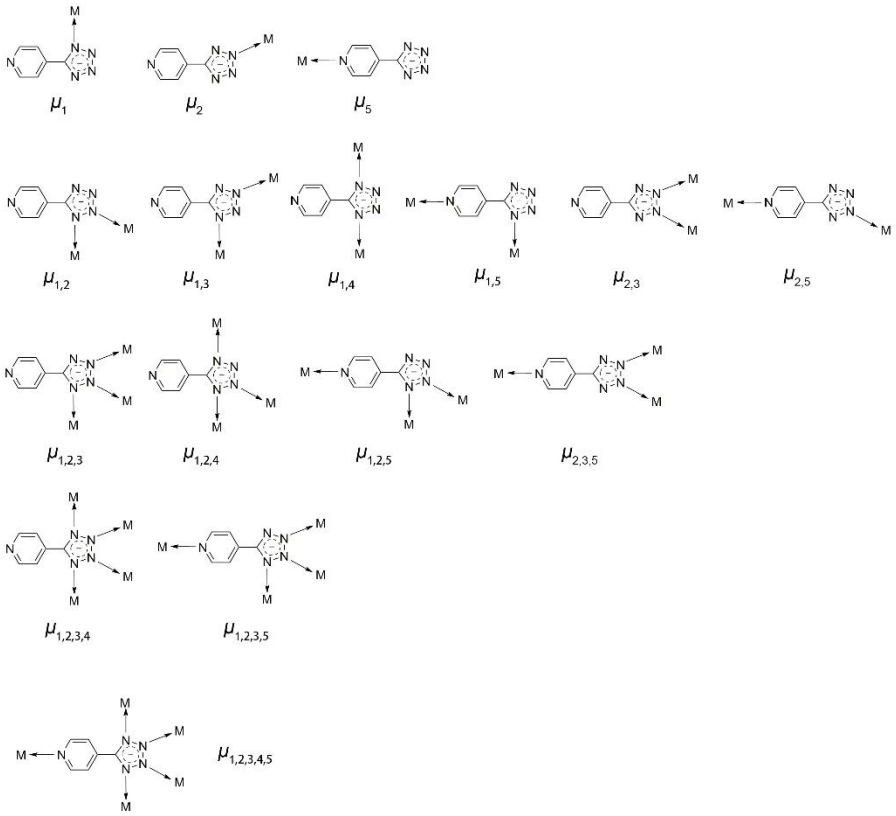

Scheme S1. The coordination modes of 4-(1H-tetrazol-5-yl)pyridine.

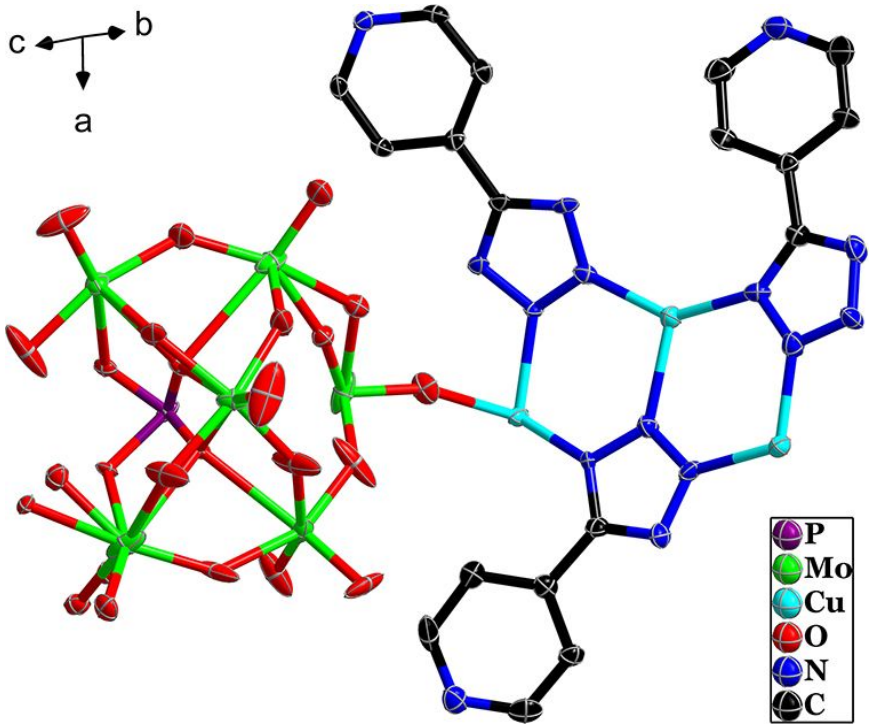

Figure S1. ORTEP drawing of POMCP **1** with thermal ellipsoids at 50% probability. Crystal water molecules and hydrogen atoms are omitted for clarity.

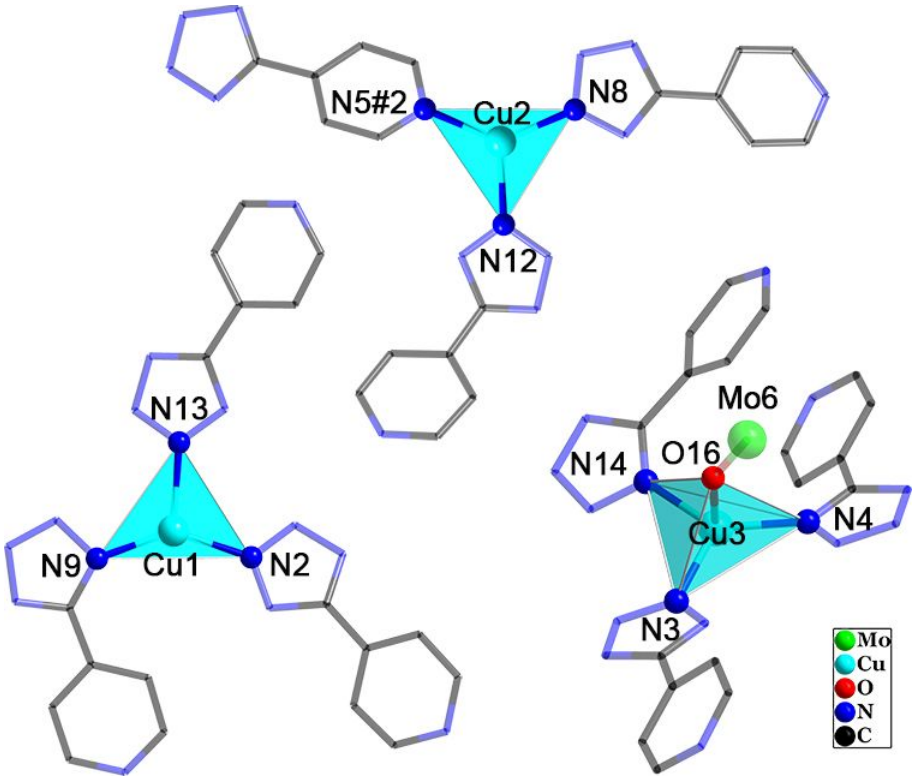

Figure S2. The coordination modes of Cu1 (bottom left), Cu2 (top), and Cu3 (bottom right) in POMCP **1**. Symmetry transformations used to generate equivalent atoms: #2: x+1, y+1, z.

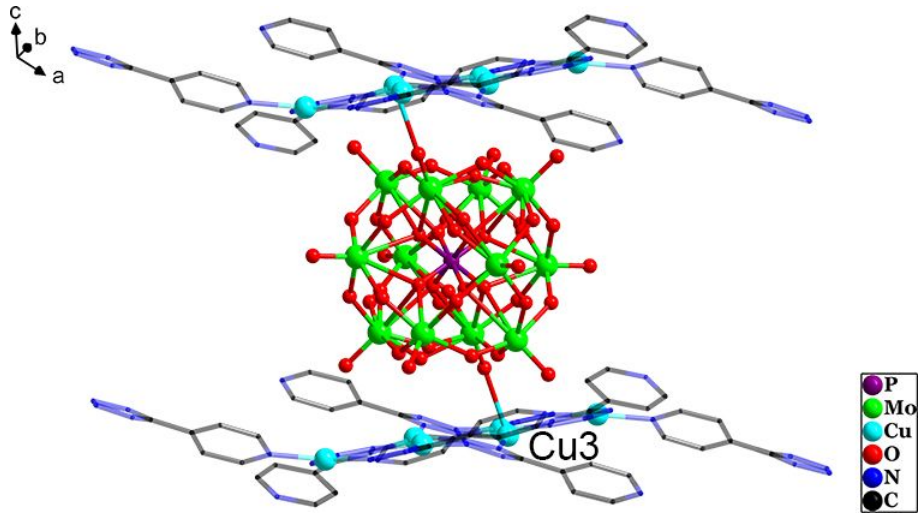

Figure S3. The coordination mode of PMo_{12} polyoxoanion in POMCP **1**.

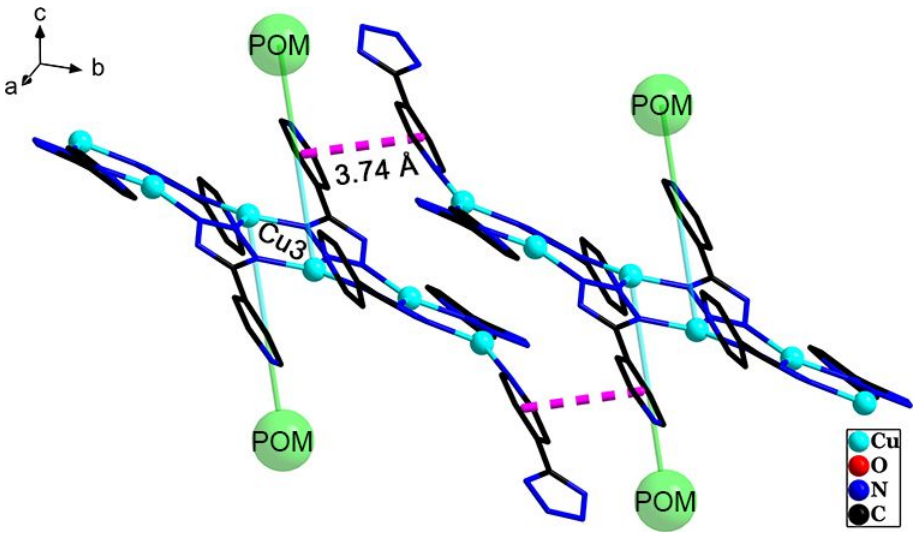

Figure S4. The π···π interaction occurring 3D stacking structure of POMCP **1**.

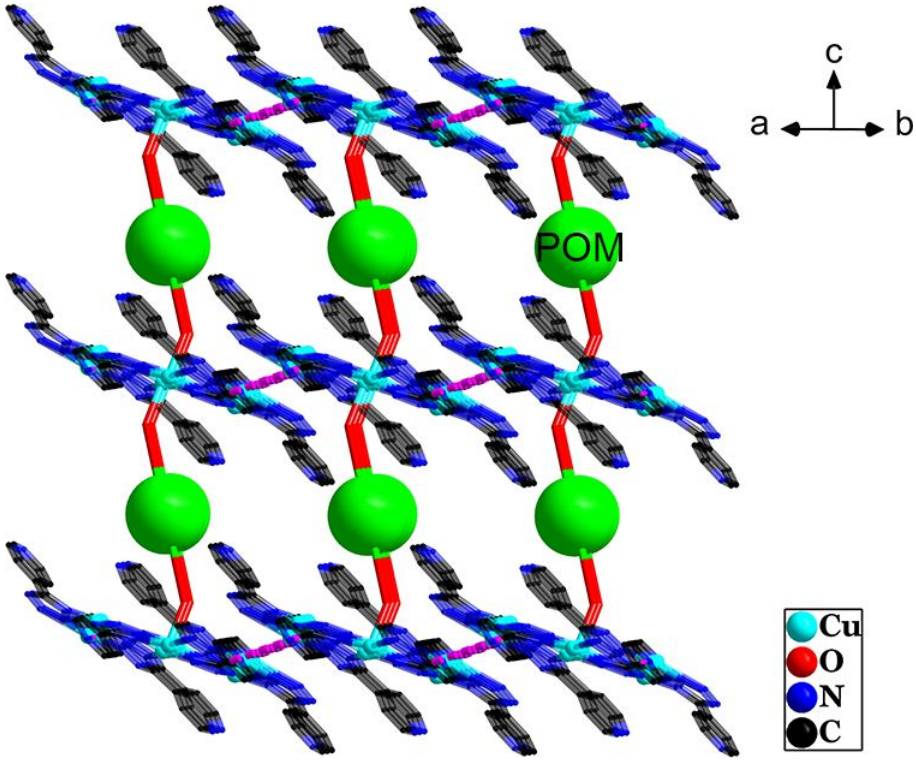

Figure S5. The 3D stacking structure via π···π interaction in POMCP **1**.

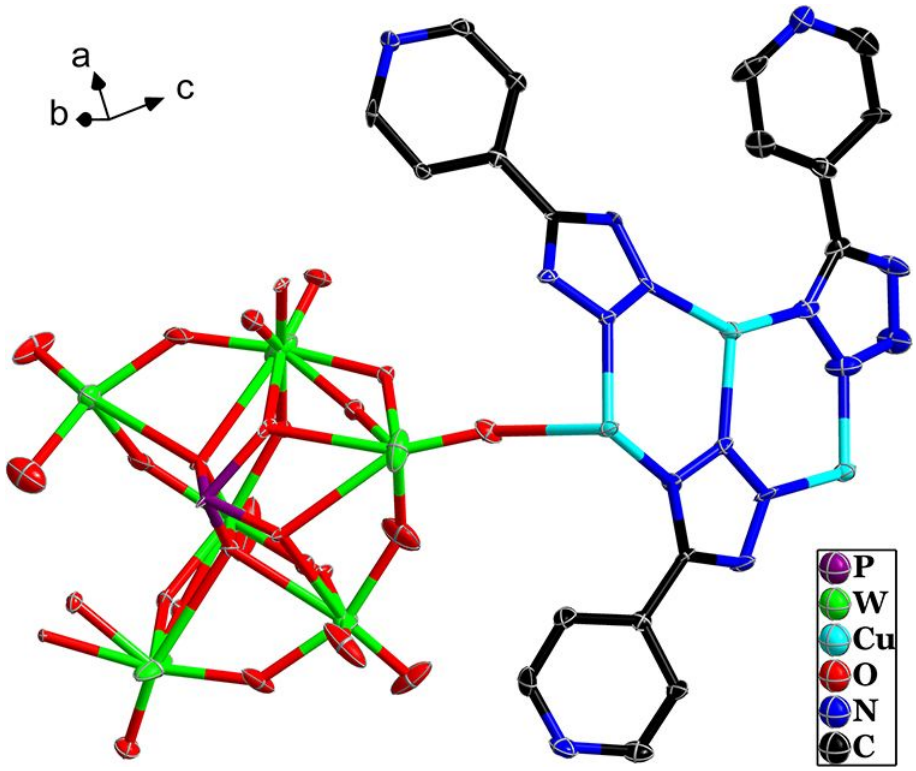

Figure S6. ORTEP drawing of POMCP **2** with thermal ellipsoids at 50% probability. Crystal water molecules and hydrogen atoms are omitted for clarity.

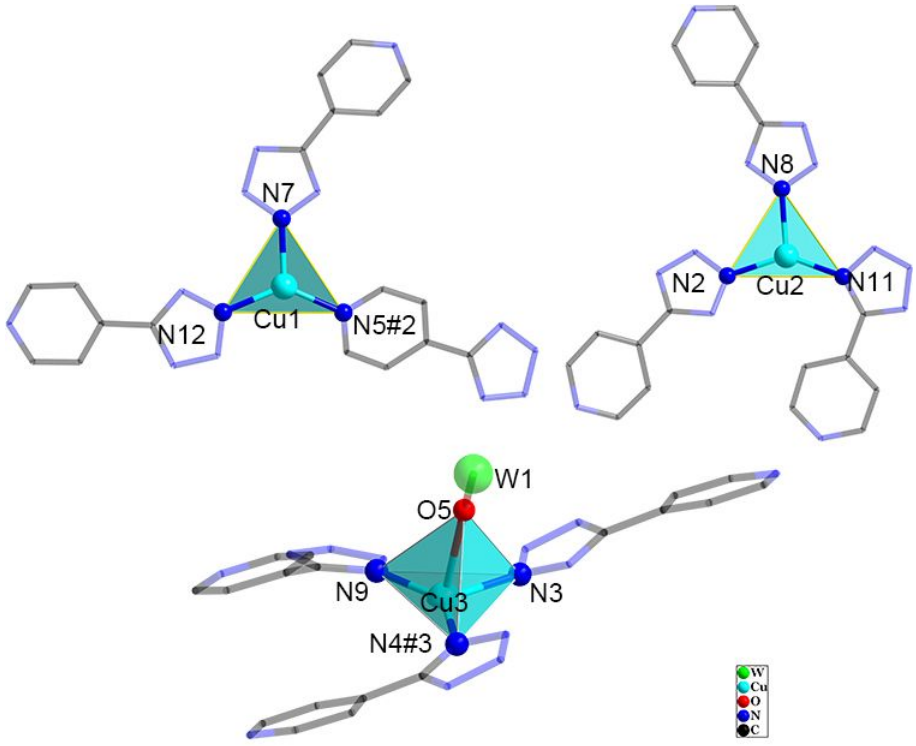

Figure S7. The coordination modes of Cu1 (top left), Cu2 (top right), and Cu3 (bottom) in POMCP **2**. Symmetry transformations used to generate equivalent atoms: #2: x-1, y-1, z; #3: -x-1, -y+2, -z.

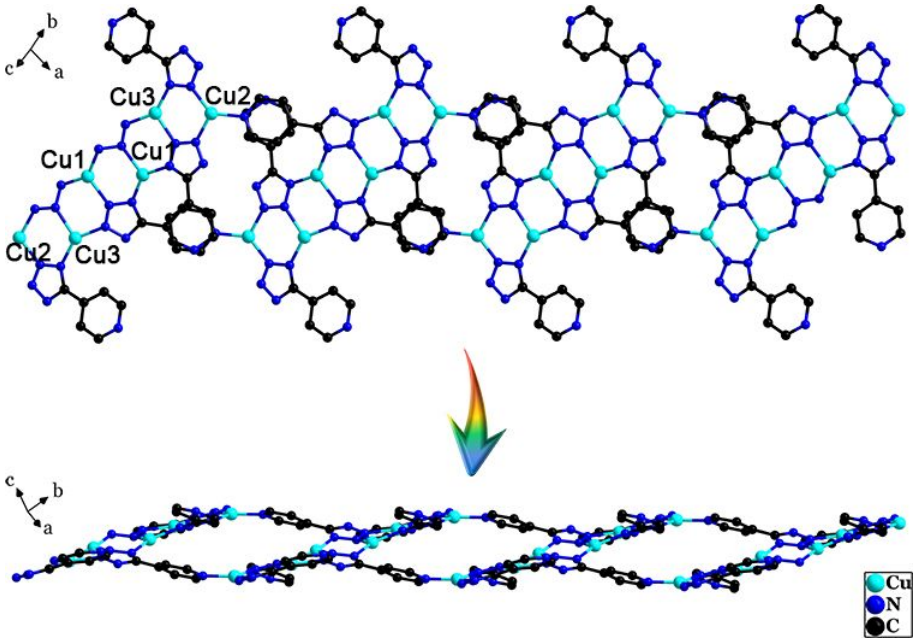

Figure S8. The 1D Cu-organic chain in POMCP **2**.

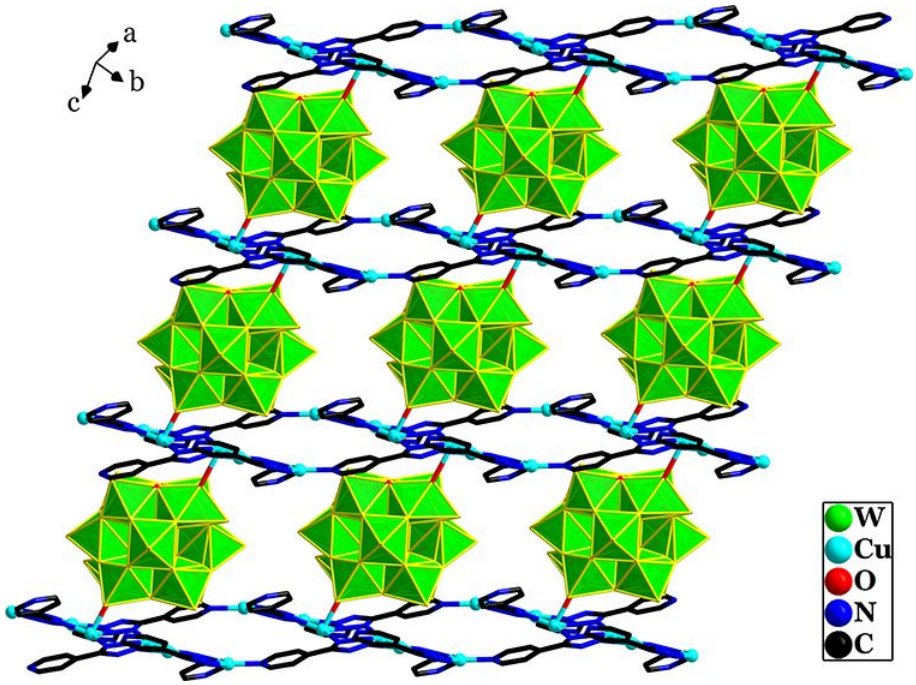

Figure S9. The 2D layer structure in POMCP **2**.

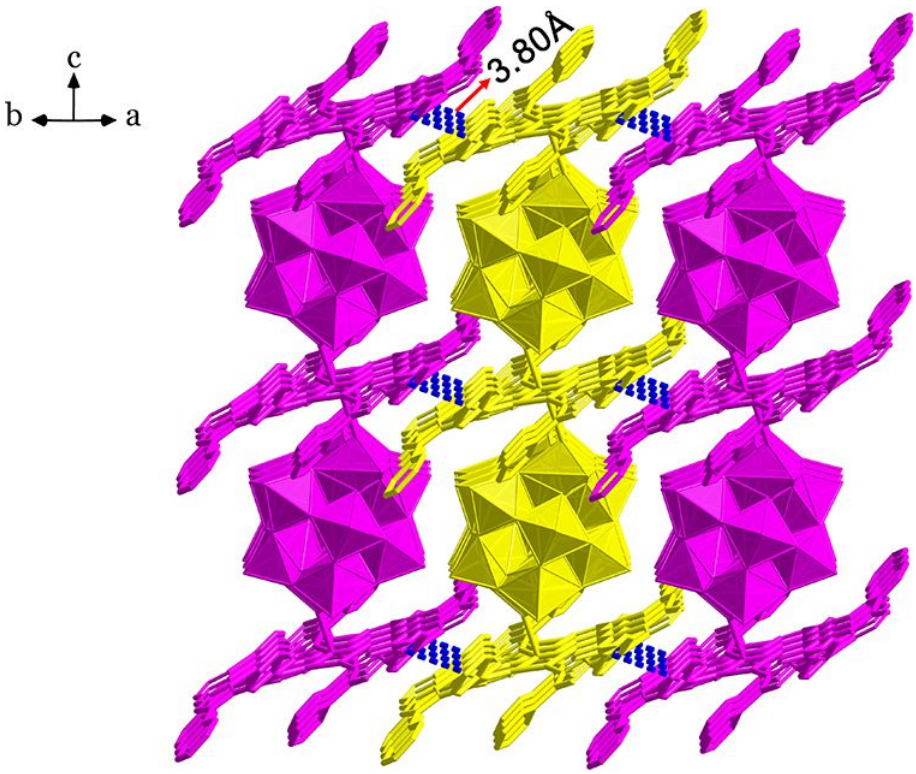

Figure S10. The 3D stacking structure via π···π interaction in POMCP **2**.

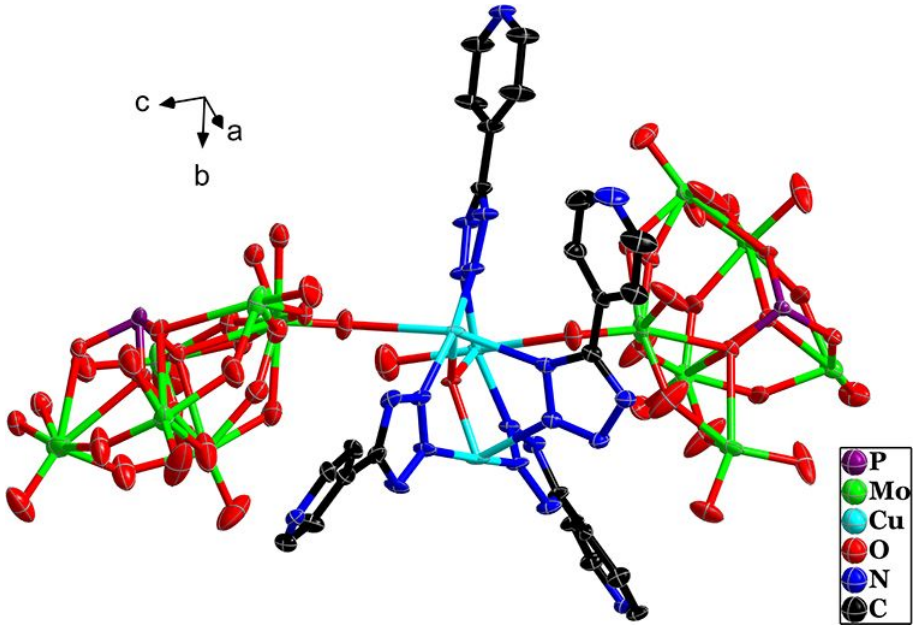

Figure S11. ORTEP drawing of POMCP **3** with thermal ellipsoids at 50% probability. Crystal water molecules and hydrogen atoms are omitted for clarity.

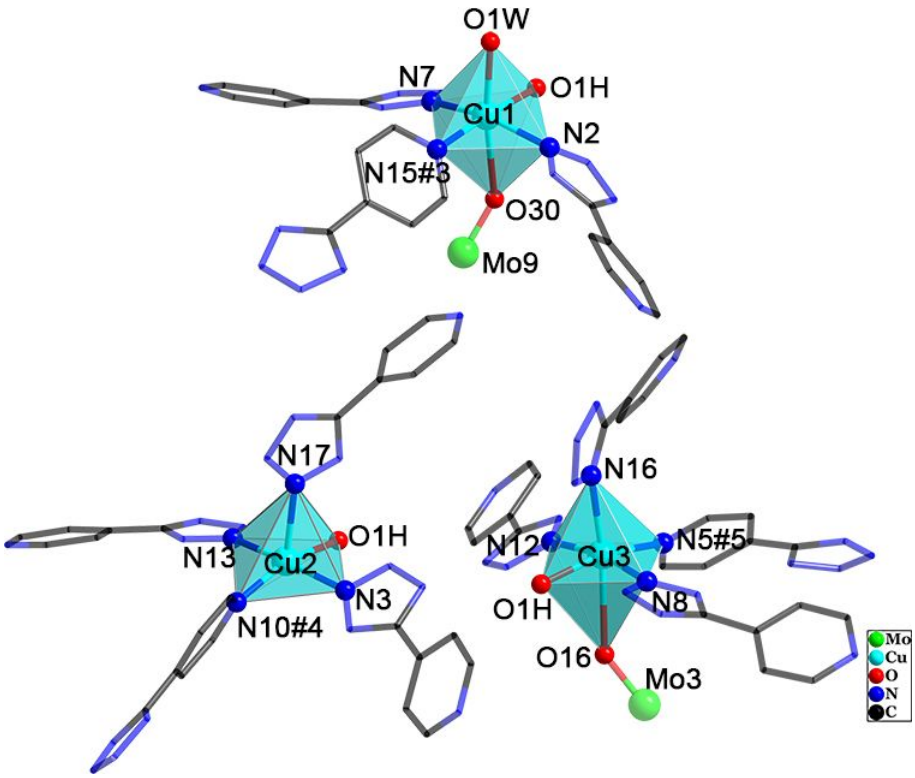

Figure S12. The coordination modes of Cu1 (top), Cu2 (bottom left), and Cu3 (bottom right) in POMCP **3**. Symmetry transformations used to generate equivalent atoms: #3: x+1, y-1, z; #4: x, y+1, z; #5: x-1, y, z; W: water molecule oxygen; H: hydroxyl oxygen.

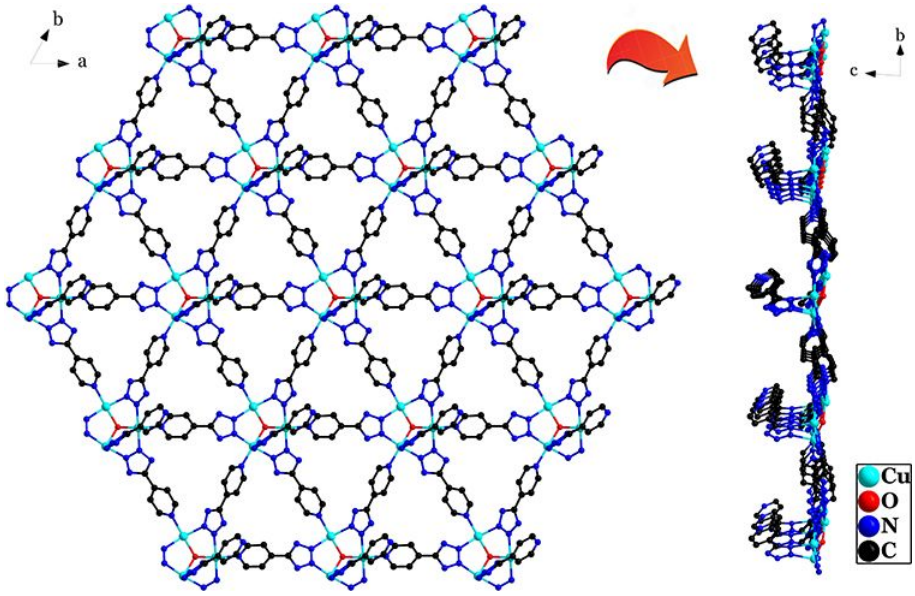

Figure S13. The 2D Cu-organic sheet in POMCP **3**.

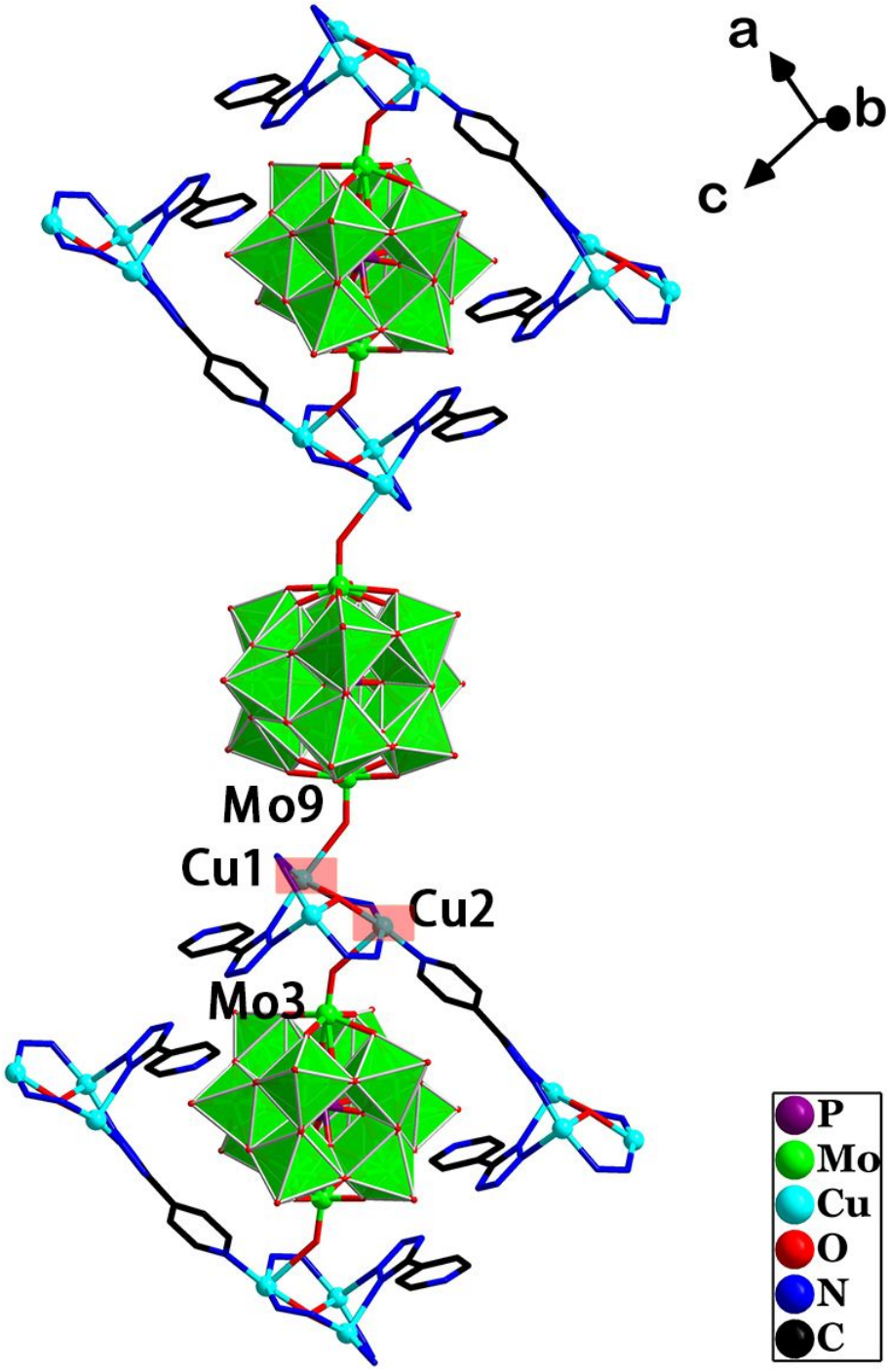

Figure S14. The coordination mode of PMo_{12} polyoxoanion in POMCP **3**.

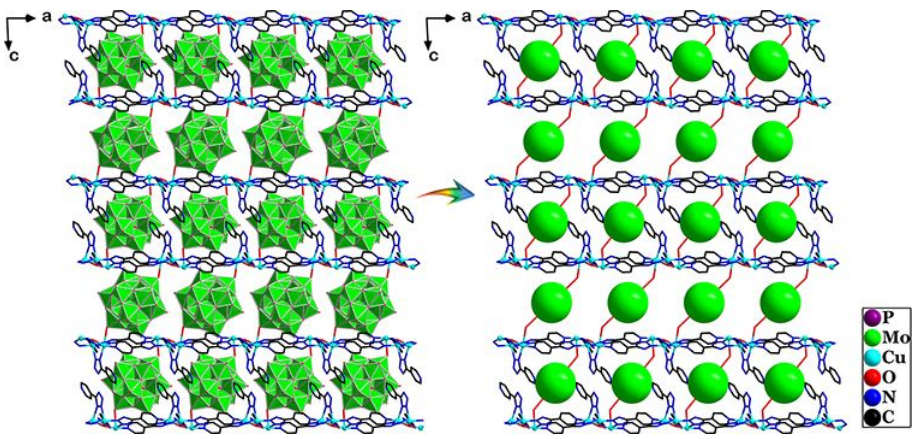

Figure S15. The 3D pillar-layered POMCP structure of POMCP **3**

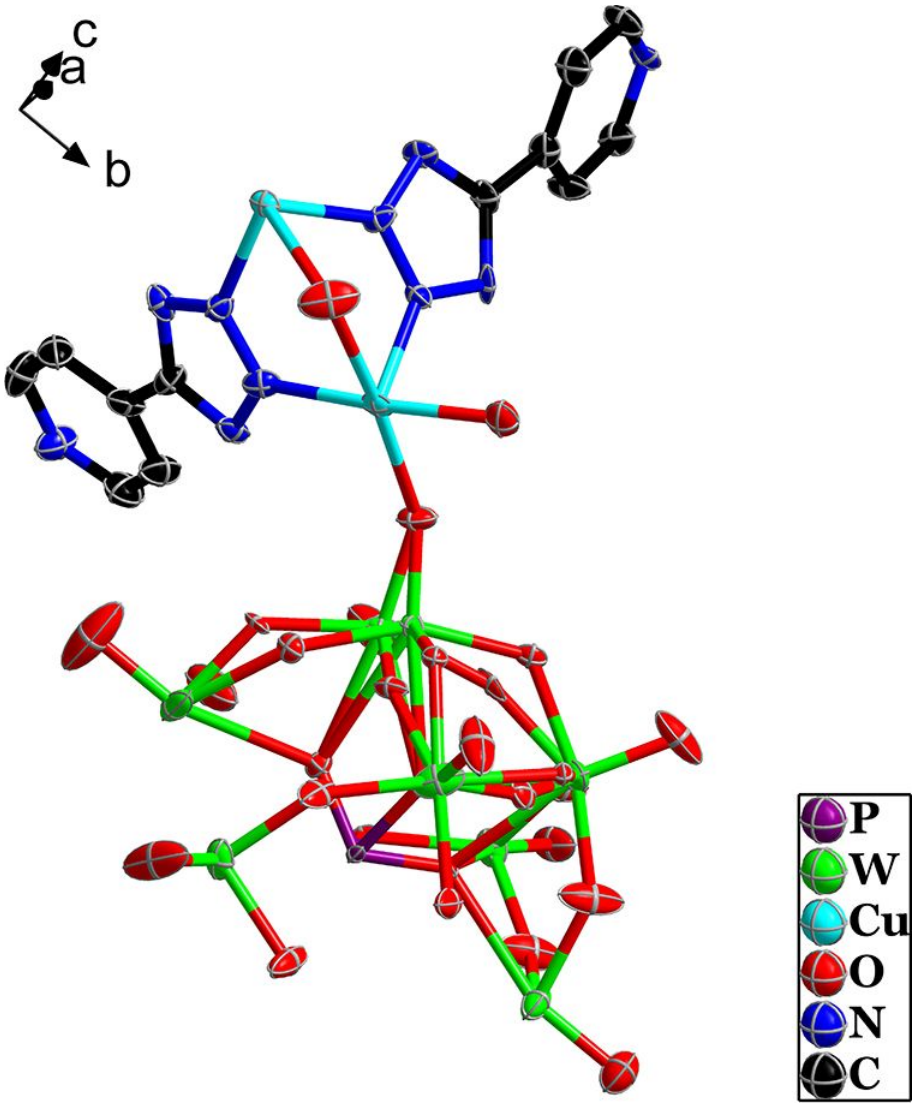

Figure S16. ORTEP drawing of POMCP **4** with thermal ellipsoids at 50% probability. Crystal water molecules and hydrogen atoms are omitted for clarity.

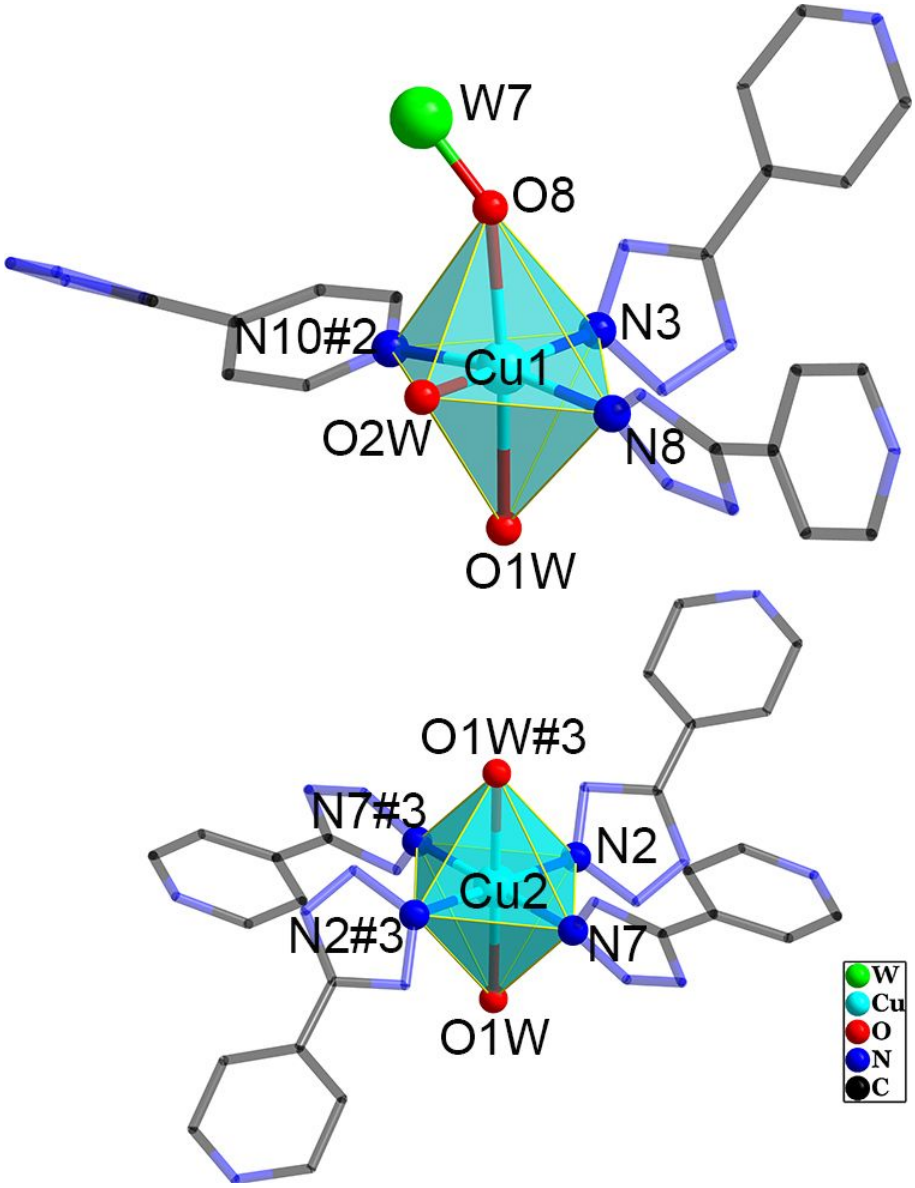

Figure S17. The coordination modes of Cu1 (top), and Cu2 (bottom) in POMCP **4**. Symmetry transformations used to generate equivalent atoms: #2 x, -y+1, z-1/2; #3 -x+3/2, -y+1/2, -z; W: water molecule oxygen.

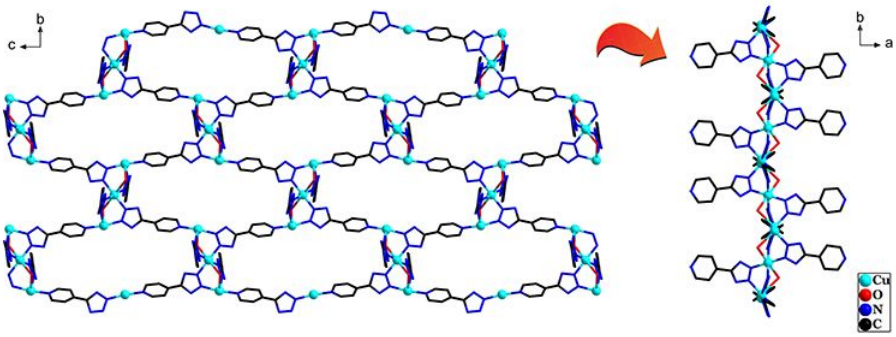

Figure S18. The 2D Cu-organic sheet in POMCP **4**.

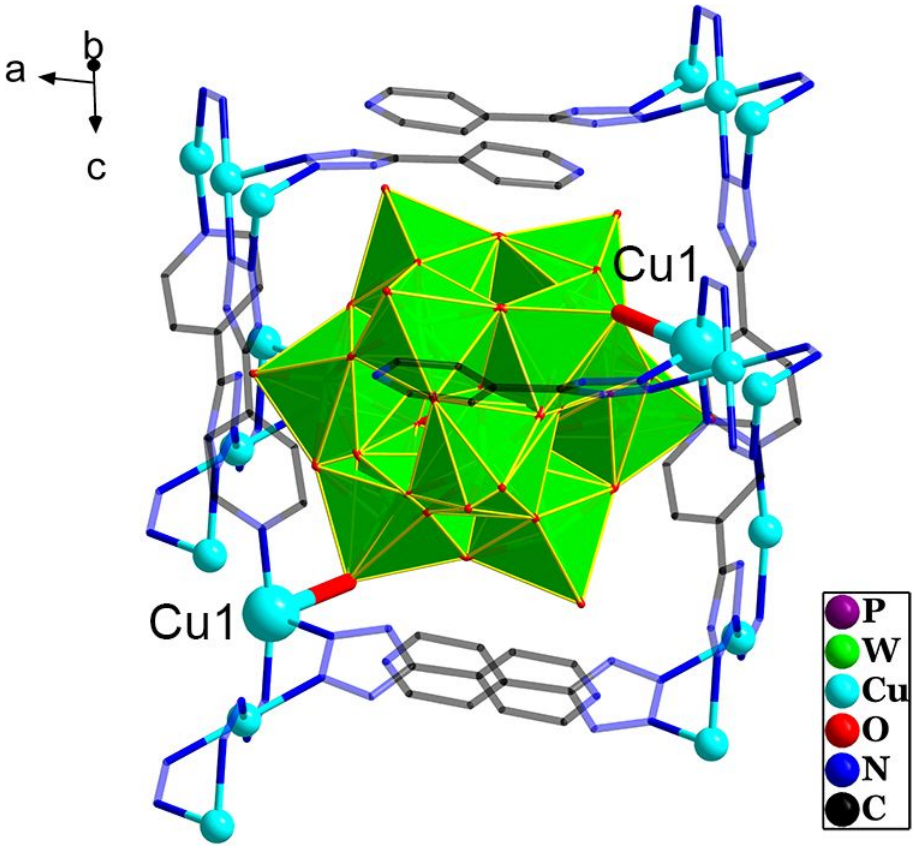

Figure S19. The coordination mode of PW_{12} polyoxoanion in POMCP **4**.

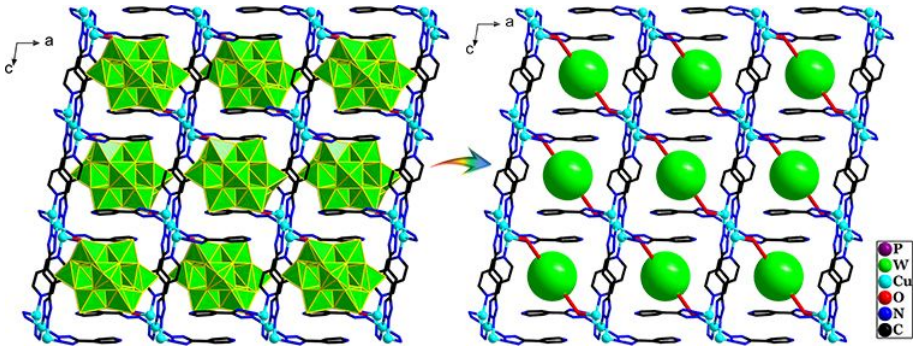

Figure S20. The 3D pillar-layered POMCP structure of POMCP **4**

III. Supplementary Physical Characterizations

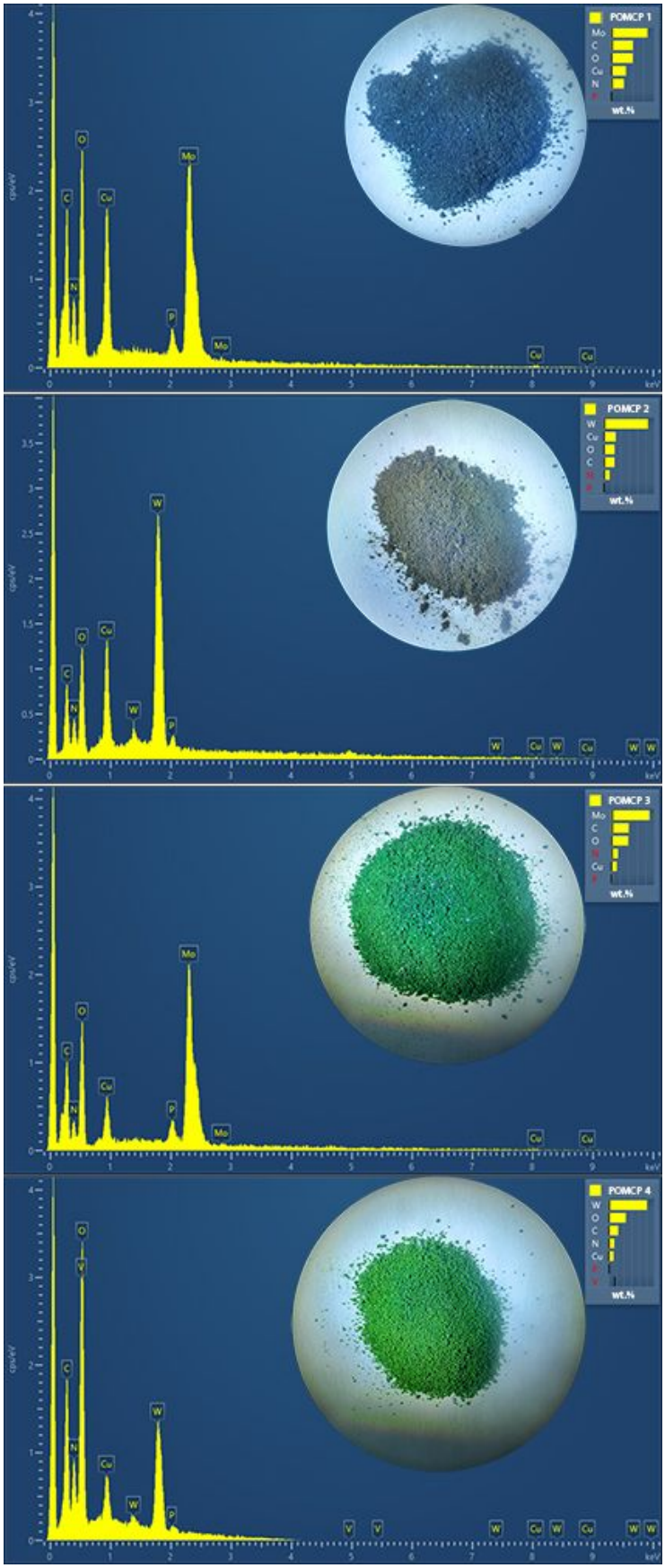

Figure S21. The EDS measurement and macromorphology of POMCPs **1**-**4**.

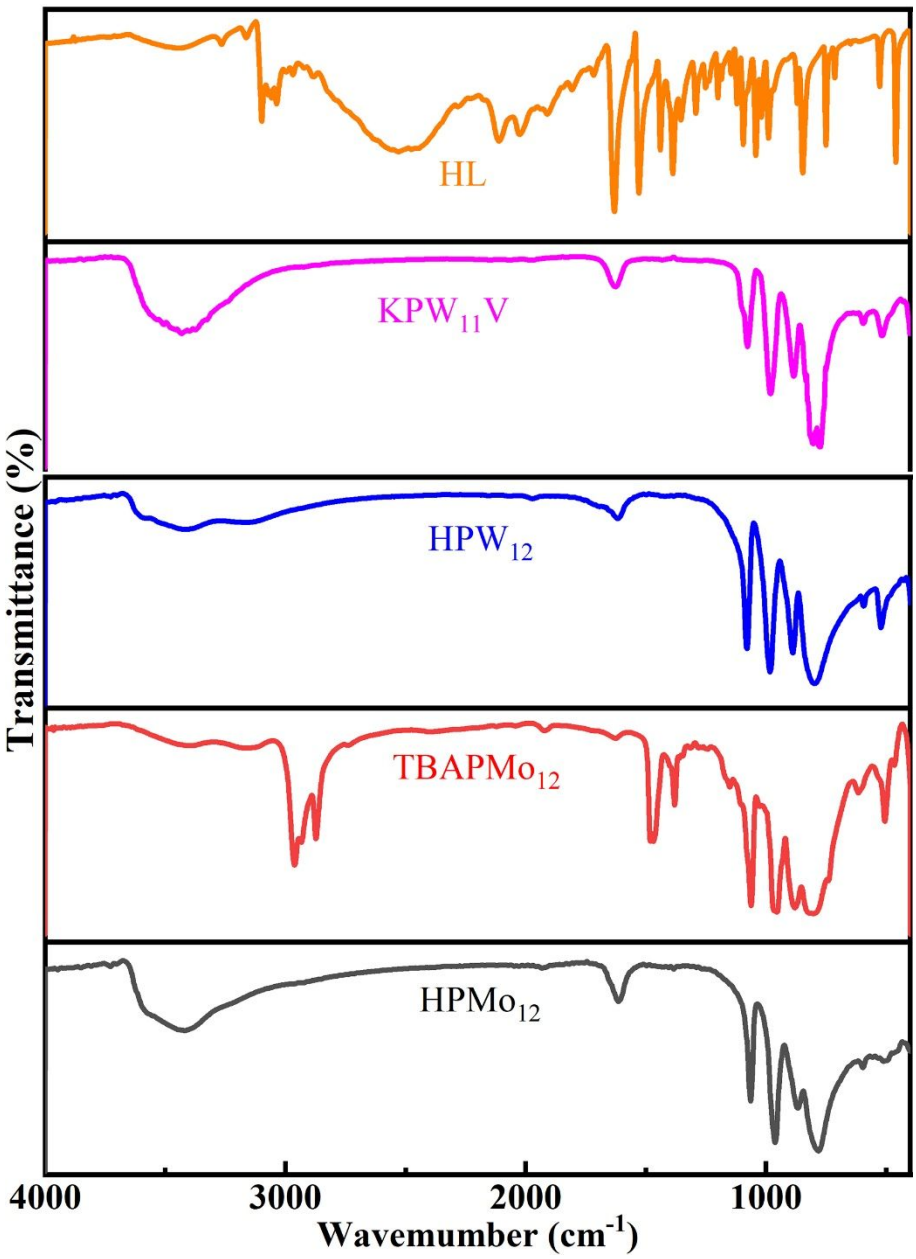

Figure S22. IR spectra for POM precursors and 4-(1H-tetrazol-5-yl)pyridine.

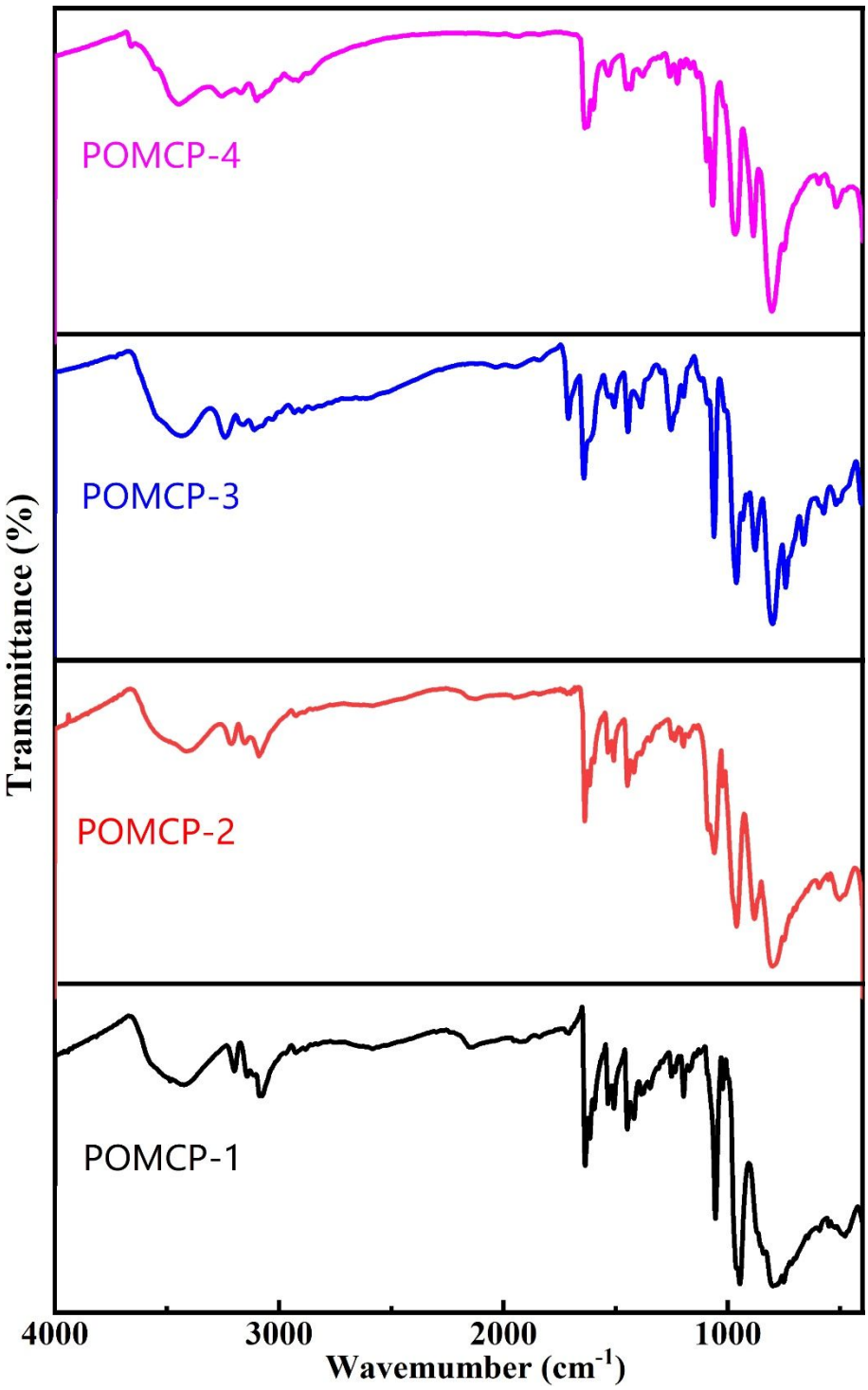

Figure S23. IR spectra for POMCPs **1-4**.

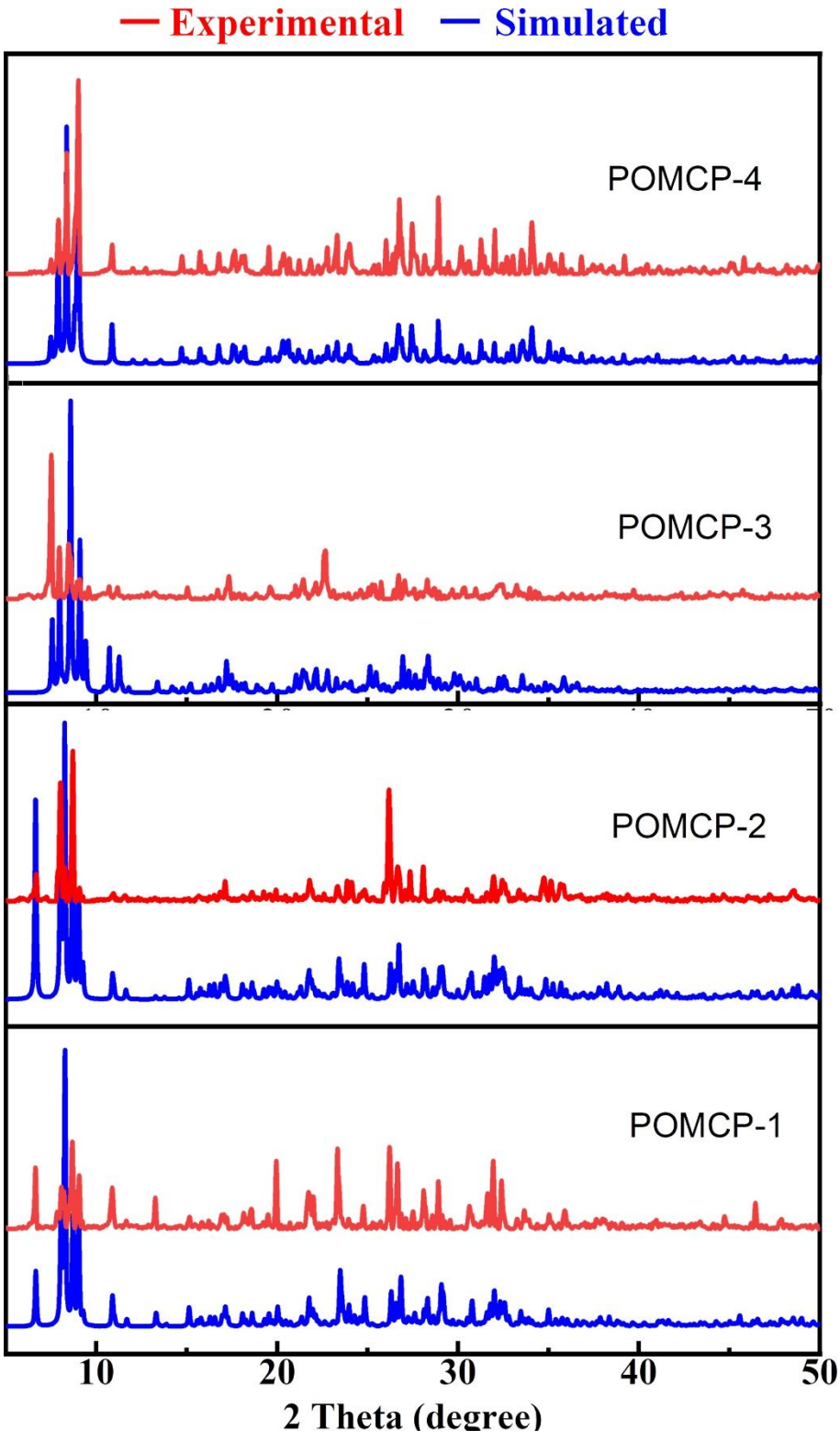

Figure S24. The simulated and experimental PXRD patterns for POMCPs **1-4**.

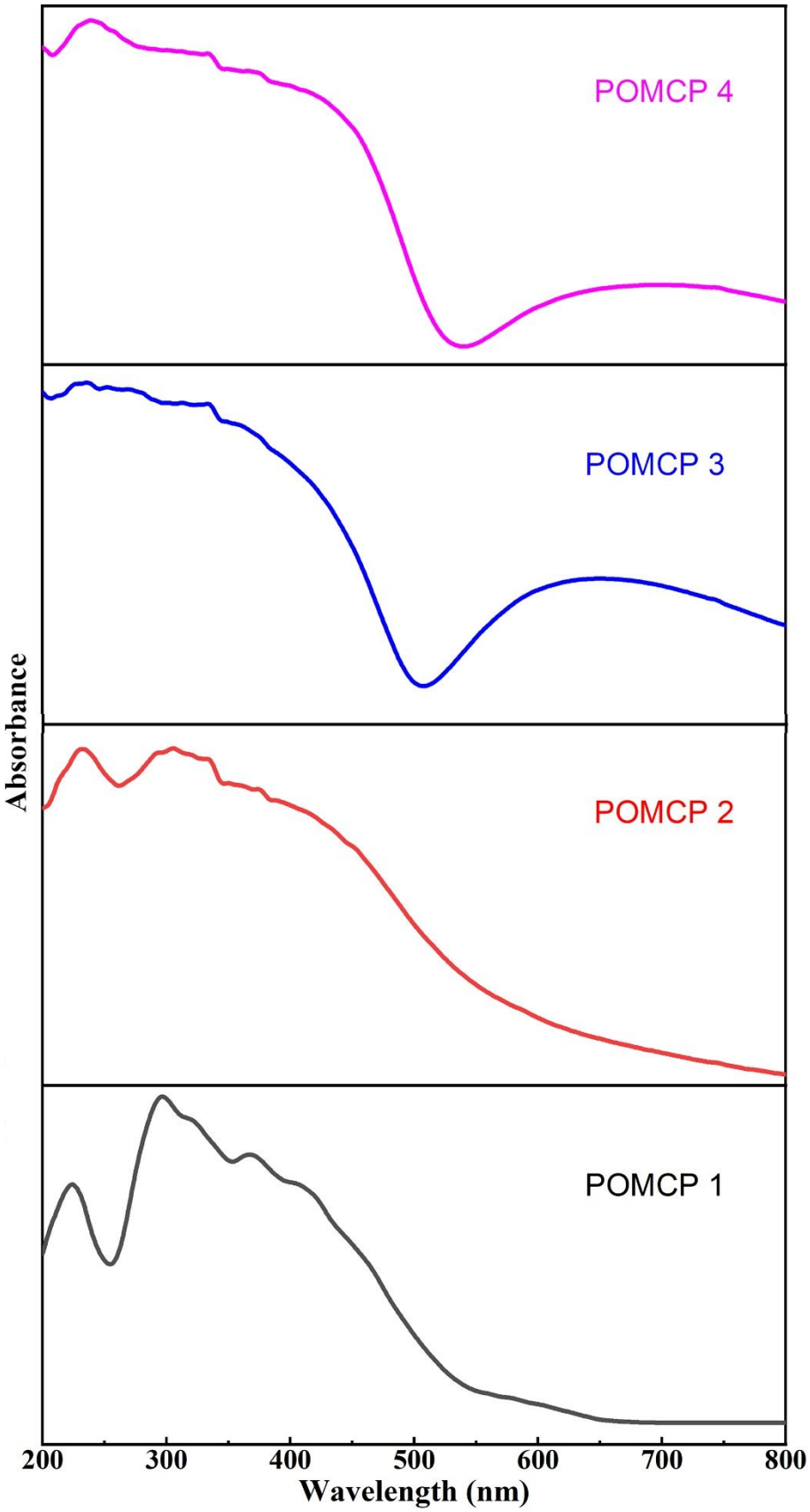

Figure S25. UV−vis diffuse reflectance spectra of POMCPs **1-4**.

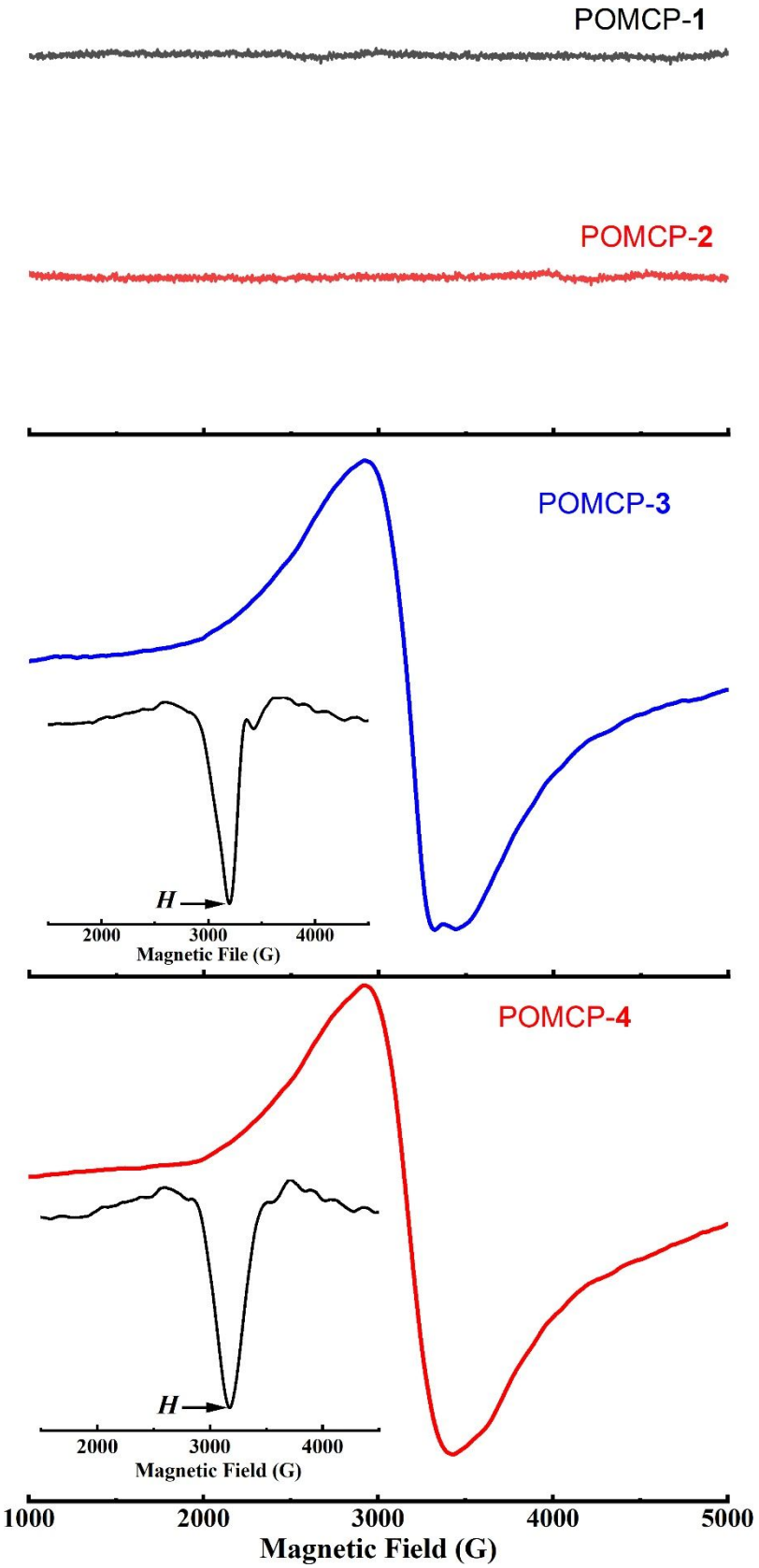

Figure S26. Room temperature solid state EPR spectra of POMCPs **1-4**. The inset is the first order differential curve of the corresponding spectra, and the *H* point is the observation point.

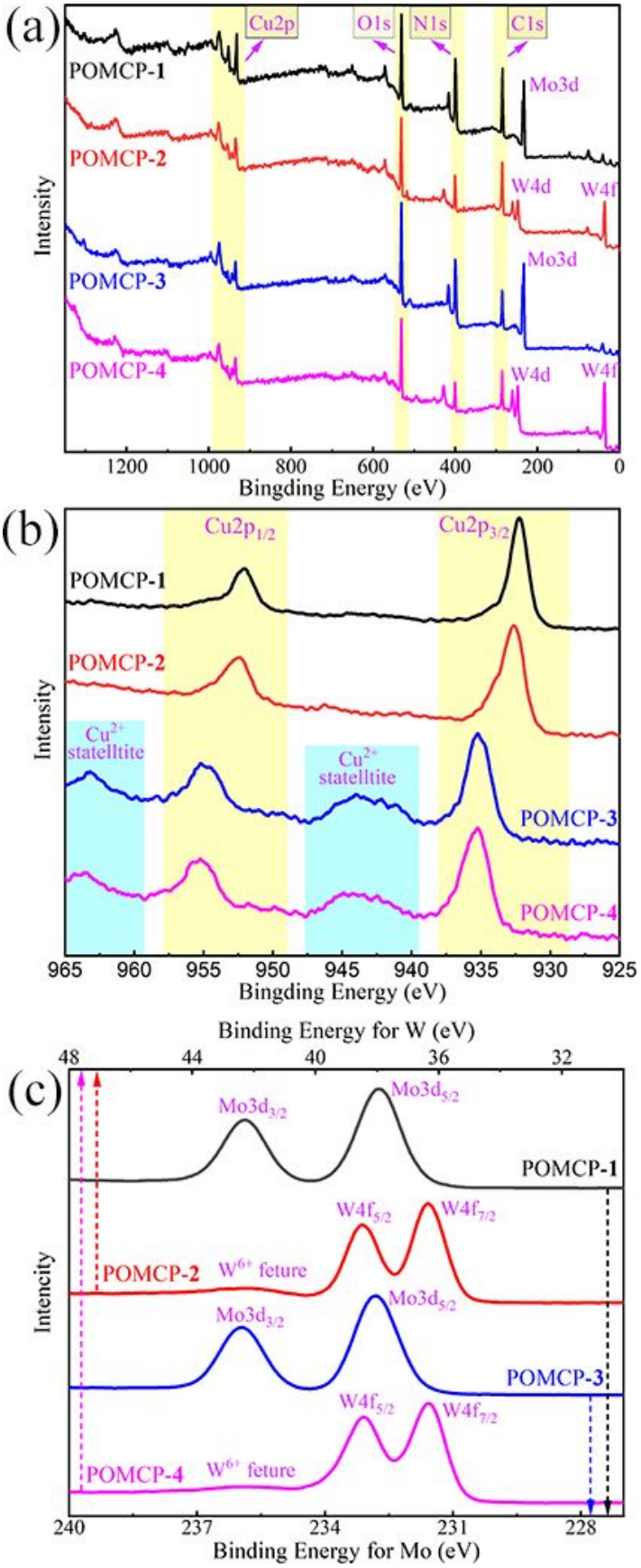

Figure S27. (a) XPS full spectra, (b) high-resolution scan of Cu2p electron, and (c) high-resolution scan of Mo3d/W4f electron for POMCPs **1-4**.

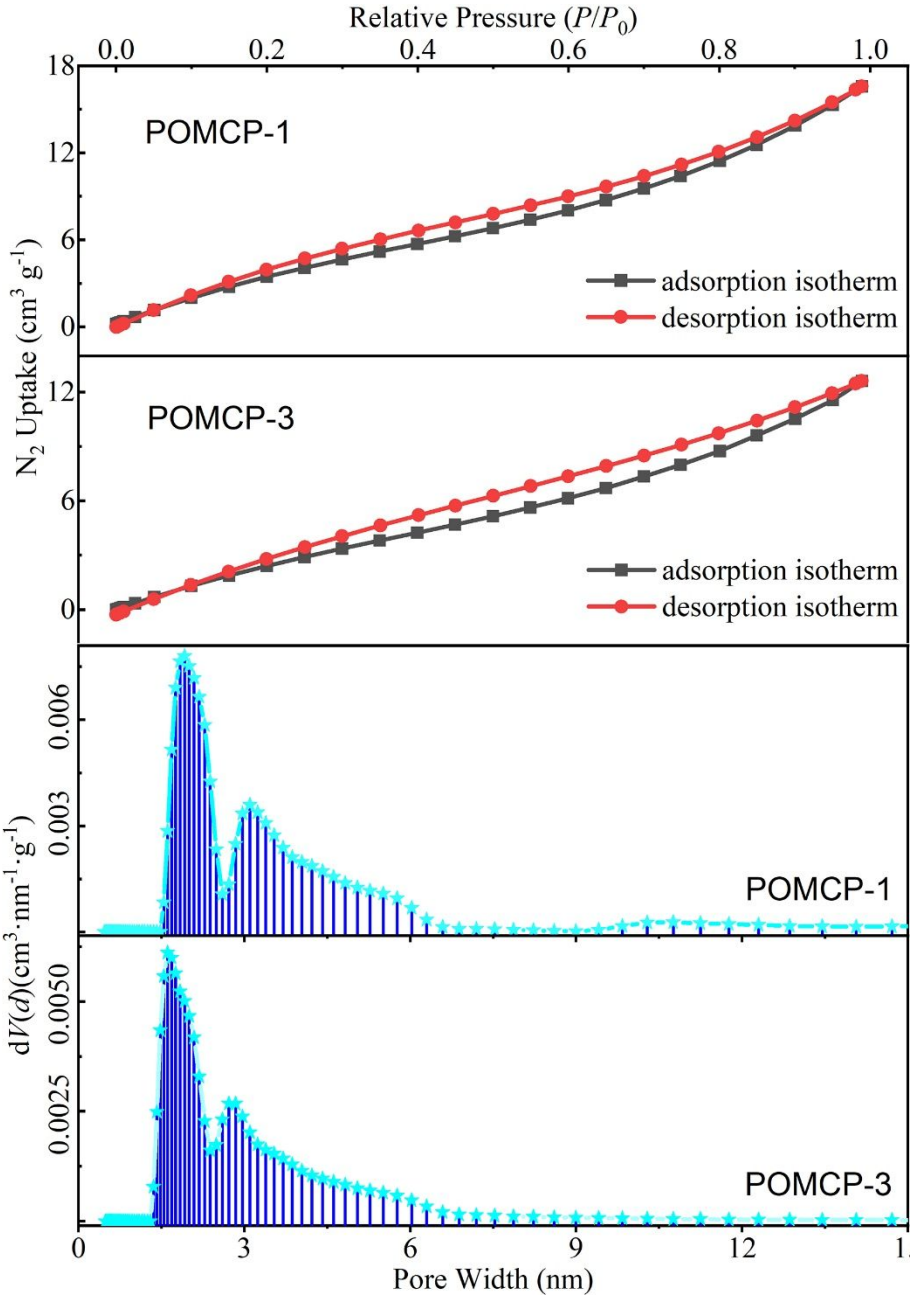

Figure S28. N_2 adsorption-desorption isotherms and the corresponding pore size distribution of POMCPs **1** and **3**.

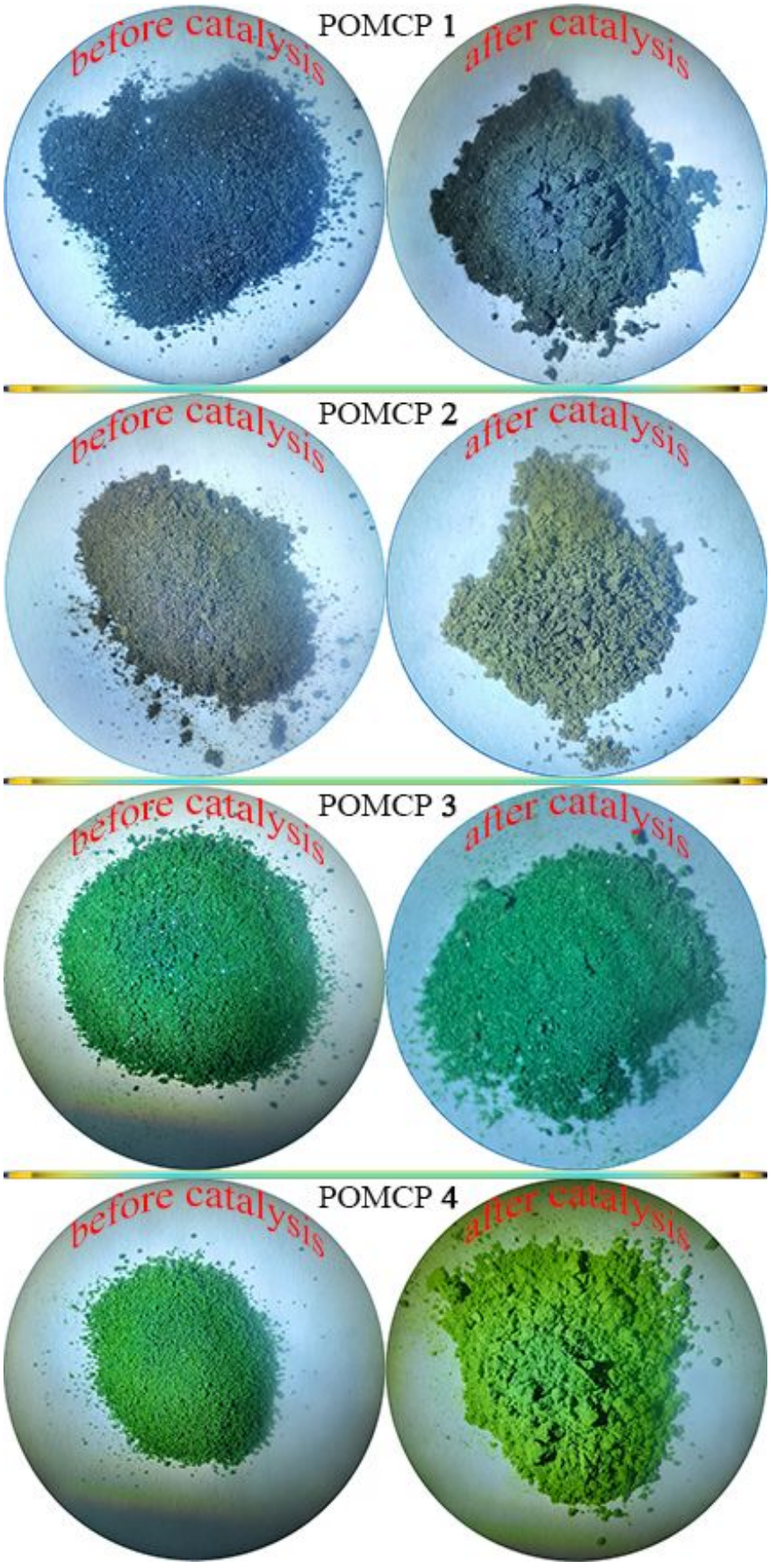

Figure S29. The morphology and color of POMCPs **1**-**4** before and after catalysis.

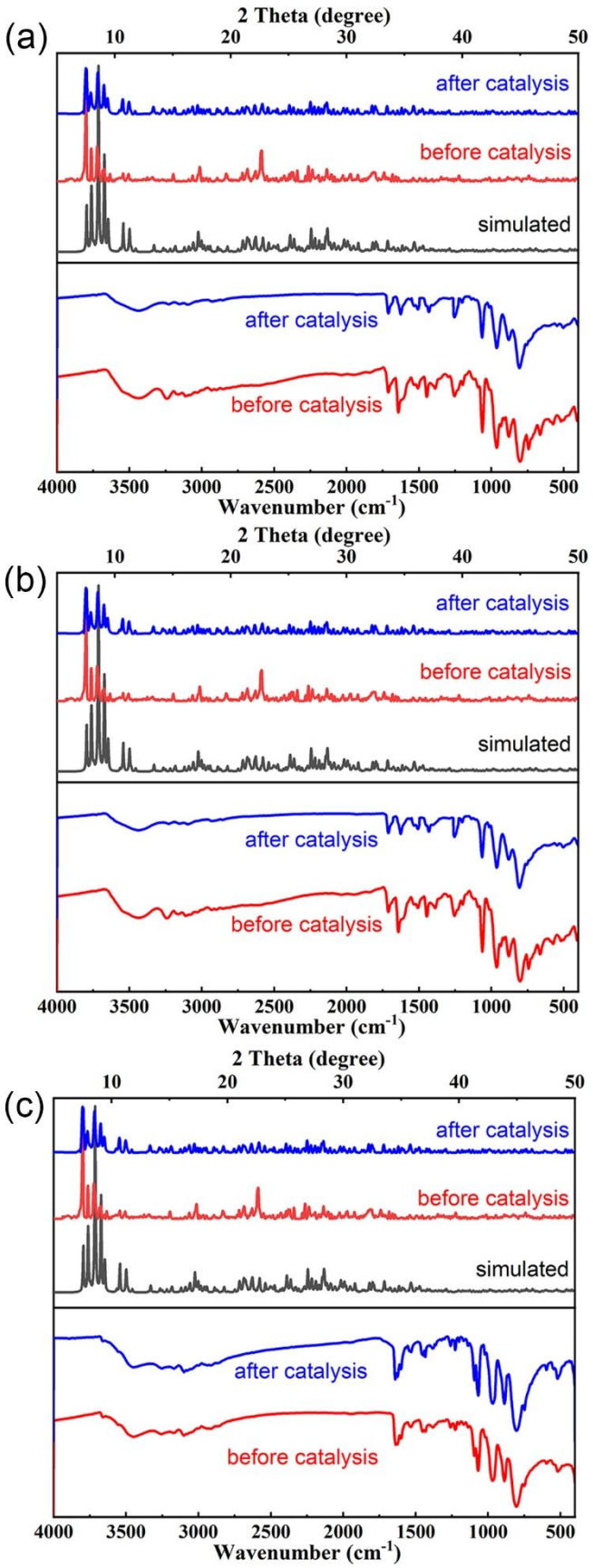

Figure S30. PXRD patterns and IR spectra for (a) POMCP **2**, (b) POMCP **3**, and (c) POMCP **4** before and after catalysis.

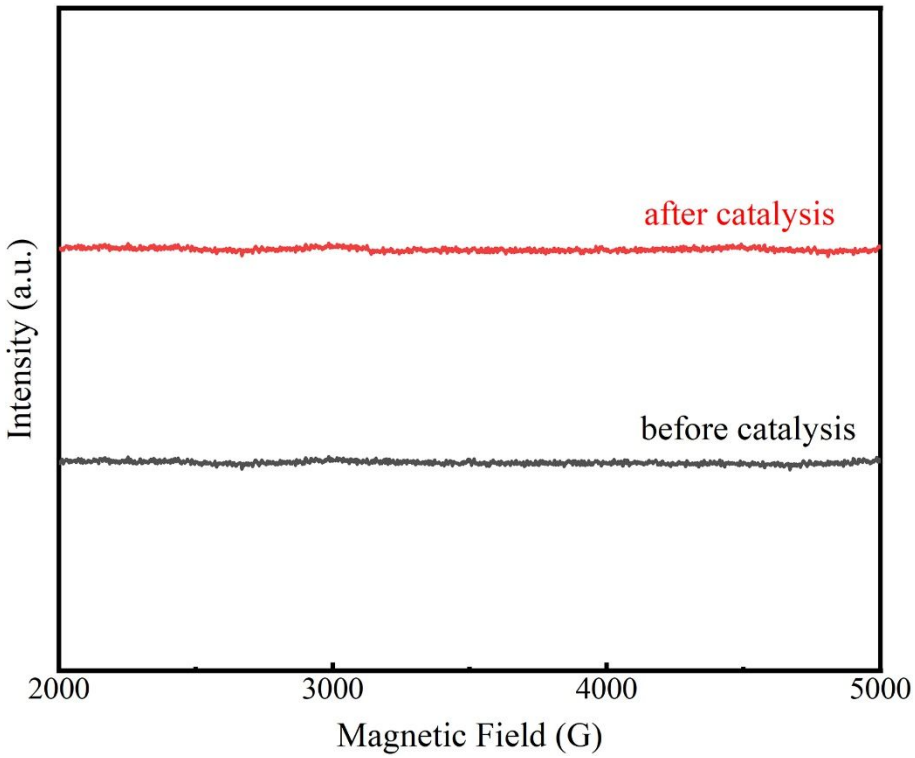

Figure S31. Room temperature solid state EPR spectra of POMCP **1** before and after catalysis.

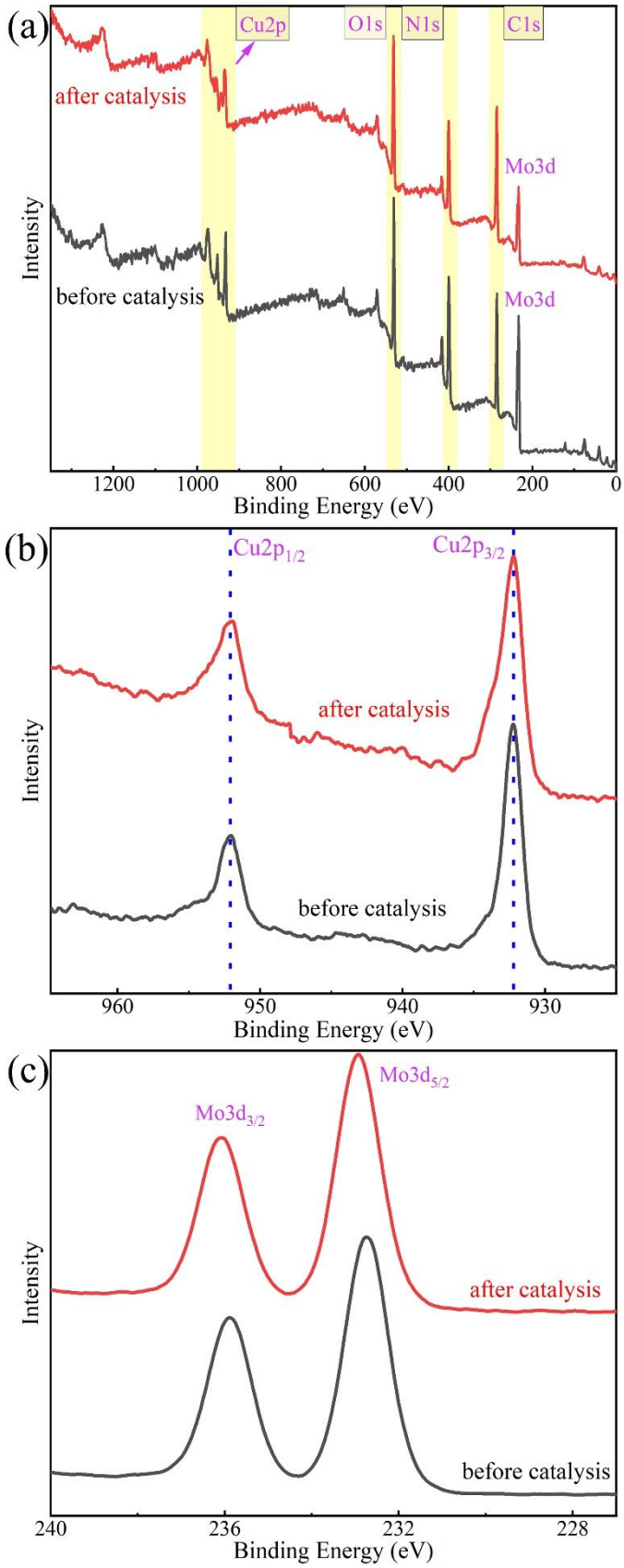

Figure S32. (a) XPS full spectra, (b) high-resolution scan of Cu2p electron, and (c) high-resolution scan of Mo3d electron for POMCP **1** before and after catalysis.

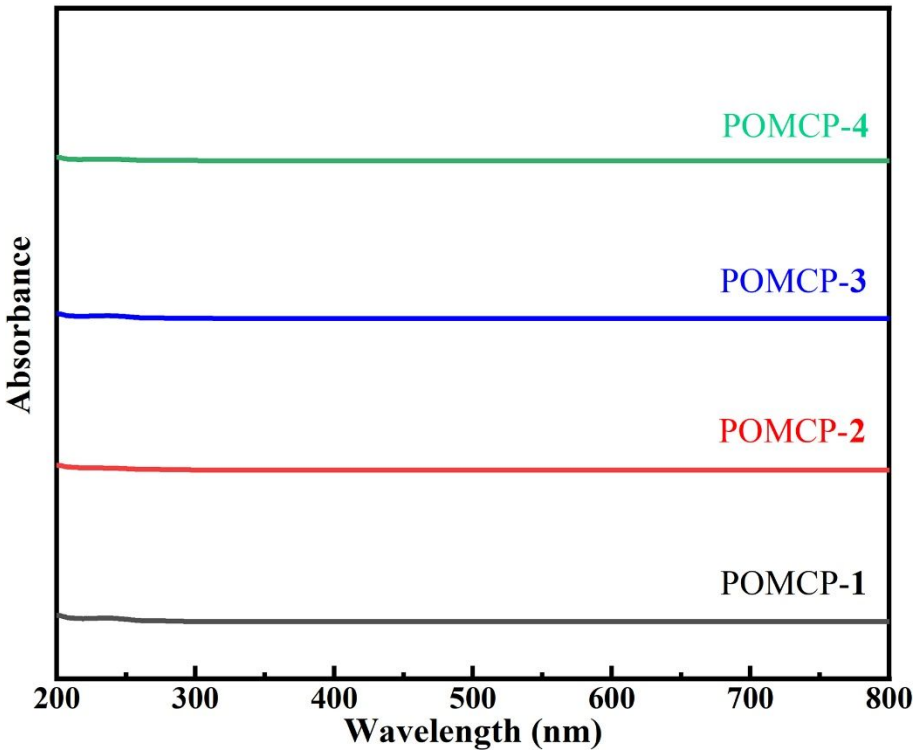

Figure S33. UV-vis spectra of the reaction solution after removing POMCPs **1**-**4**.

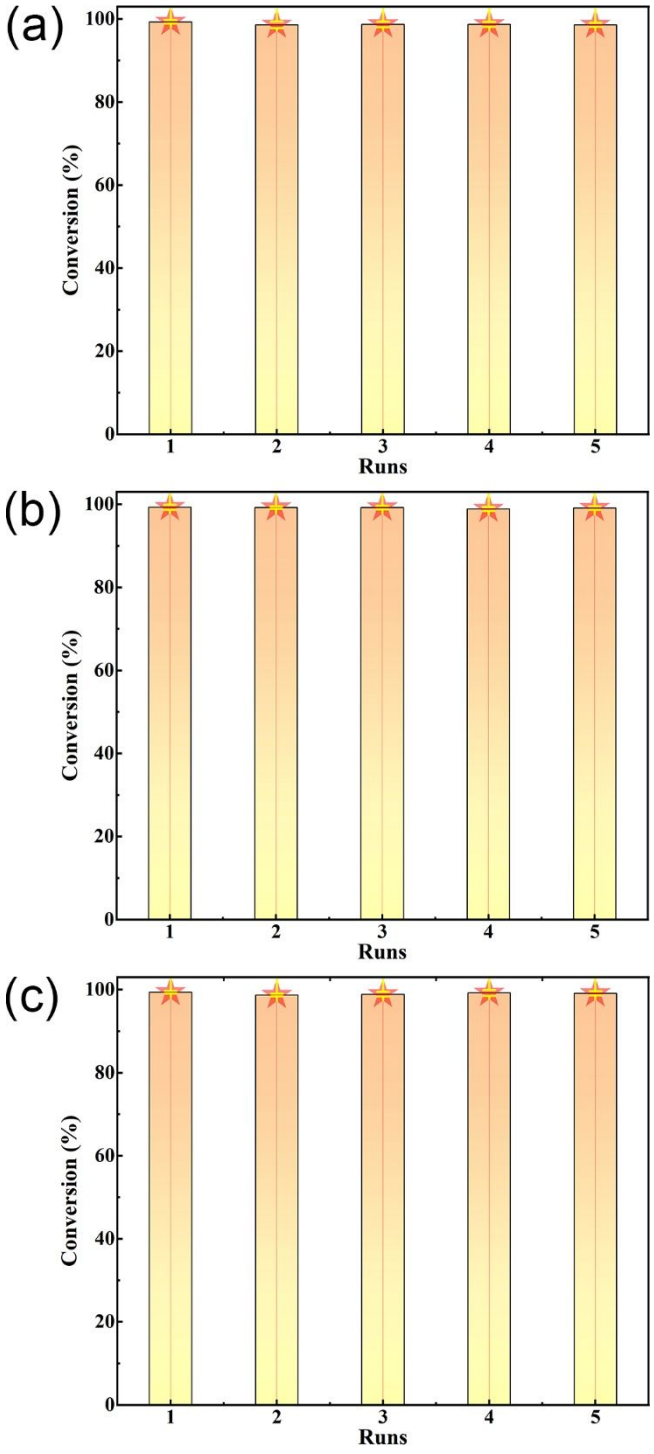

Figure S34. Cycling stability of catalysts (a) POMCP **2**, (b) POMCP **3**, and (c) POMCP **4** at almost full conversion of TMP.

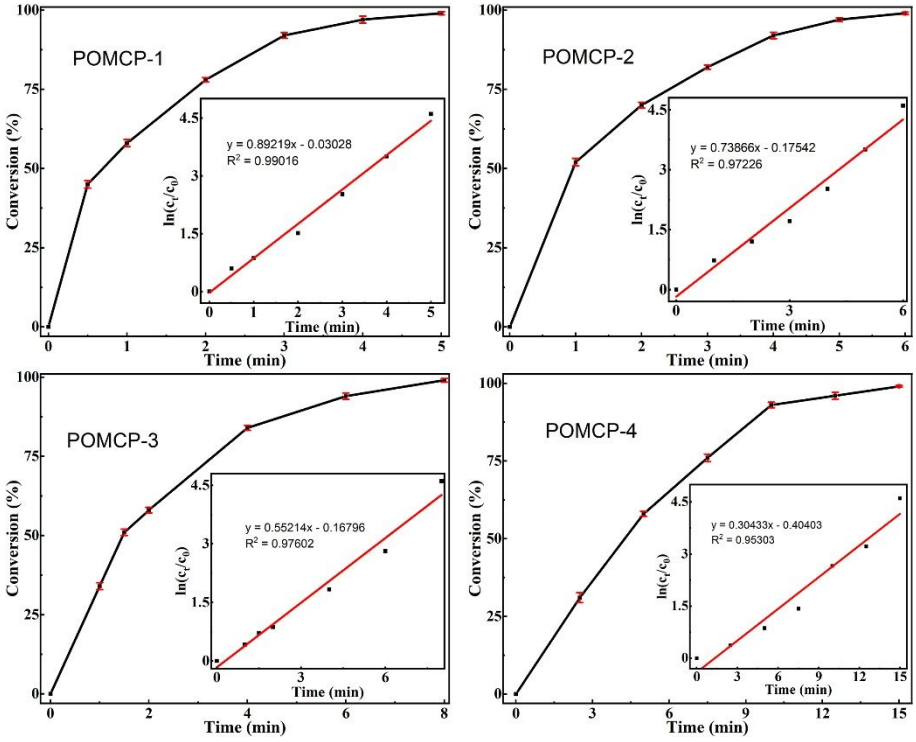

Figure S35. Time profile curves and first order kinetics fitting curves (inset graph) for the oxidation of TMP using POMCPs **1**−**4**. As can be seen from the curves, the oxidation of TMP catalyzed by POMCPs **1**−**4** is closed to the first order reaction.

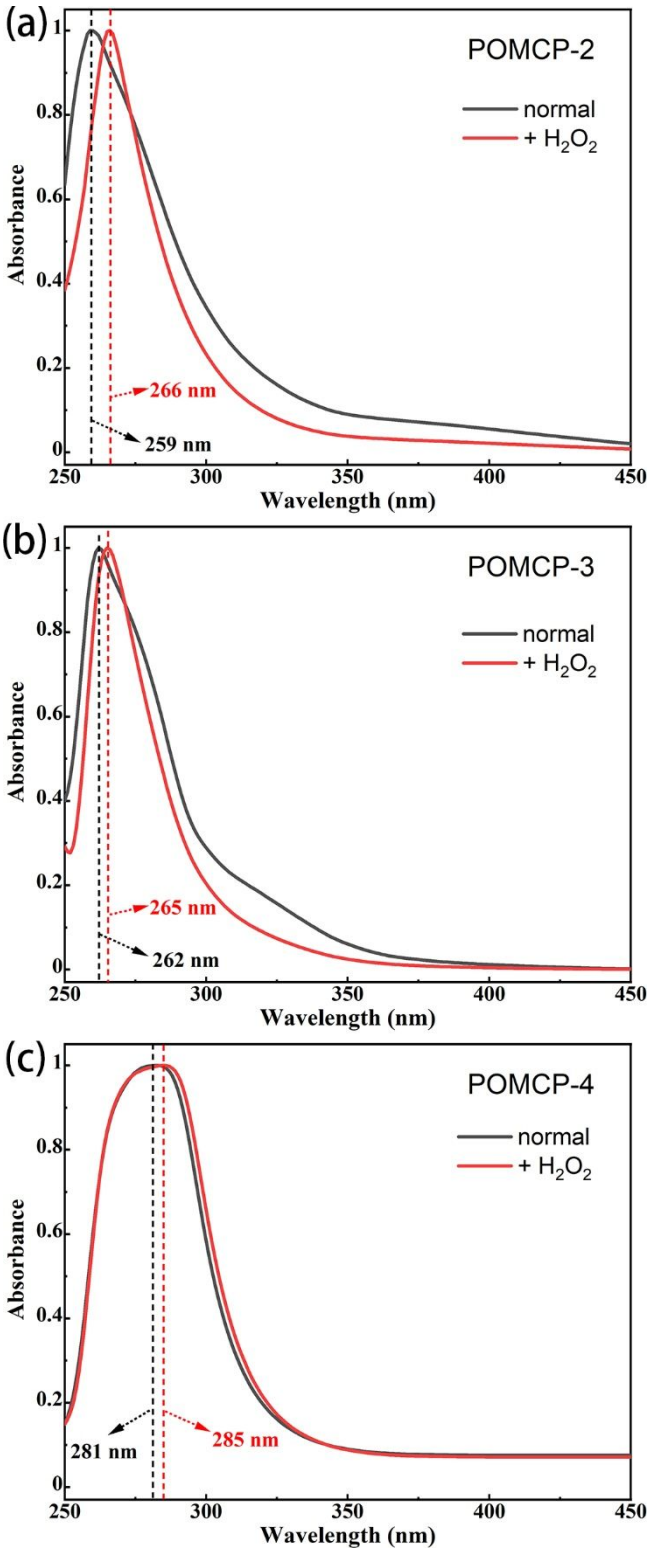

Figure S36. UV spectra of (a) POMCP **2**, (b) POMCP **3**, and (c) POMCP **4** in TMP oxidation with one-drop portions of H_2O_2 in DMSO solution.

IV. Supplementary Tables

Table S1. The Values of BVS Calculations about P, W and Cu in POMCPs 1-4, Except for the Disordered Atoms.

element	POMCP **1**	POMCP **2**	POMCP **3**	POMCP **4**
P1	5.06	5.16	5.11	5.09
P2	—	—	5.04	—
W1/Mo1	6.15	6.07	6.13	6.13
W2/Mo2	6.05	6.02	6.10	6.12
W3/Mo3	6.16	6.21	6.10	6.13
W4/Mo4	6.13	5.99	6.06	disordered
W5/Mo5	6.07	6.22	6.15	6.09
W6/Mo6	5.97	6.04	6.11	disordered
W7/Mo7	—	—	5.89	disordered
W8/Mo8	—	—	6.11	—
W9/Mo9	—	—	6.15	—
W10/Mo10	—	—	6.14	—
W11/Mo11	—	—	6.11	—
W12/Mo12	—	—	6.04	—
Cu1	1.00	1.13	2.13	2.16
Cu2	1.15	1.02	2.14	2.13
Cu3	1.14	1.14	2.12	—

Table S2. Structural Summary of Crystallized POMCP for the Oxidation of TMP.

catalyst	POM-based CPs	dimension	POM	coordination geometry of Cu	TMBQ yield (%)	TOF (h^{-1})
POMCP **1**[a]	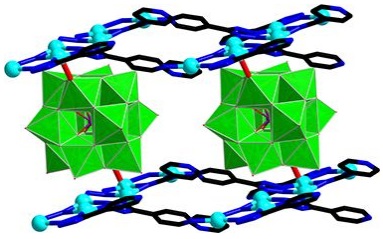	2D	$[PMo_{12}O_{40}]^{3-}$	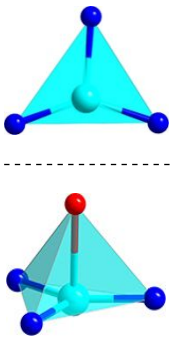	>99	2400
POMCP **2**[a]	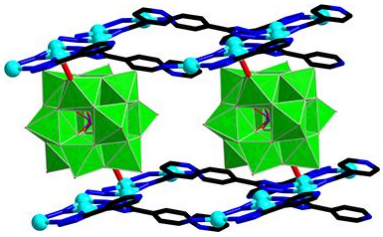	2D	$[PW_{12}O_{40}]^{3-}$	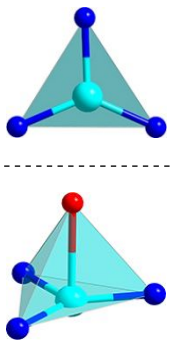	96	2000
POMCP **3**[a]	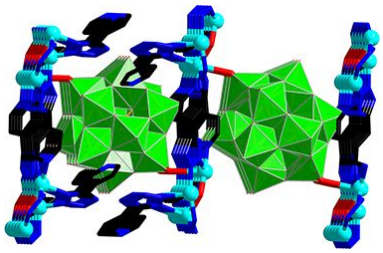	3D	$[PMo_{12}O_{40}]^{3-}$	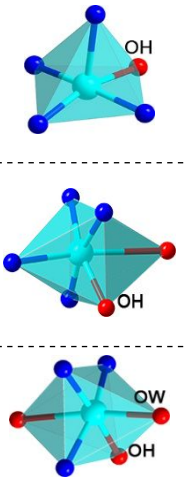	>99	1500
POMCP **4**[a]	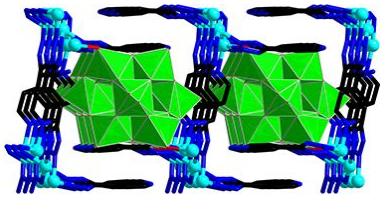	3D	$[PW_{12}O_{40}]^{3-}$	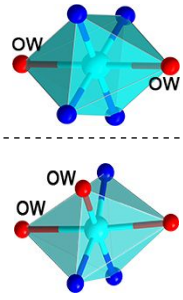	>99	800

$PWCu_4$[b]	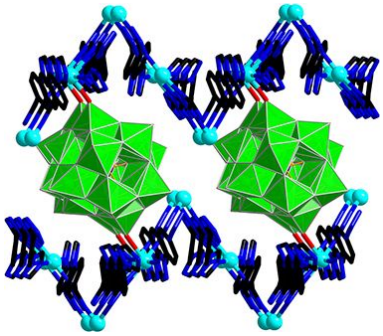	3D	$[PW_{12}O_{40}]^{3-}$	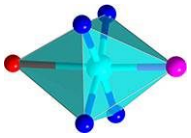 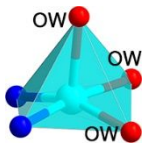	>99	394
$PWCu_7$[b]	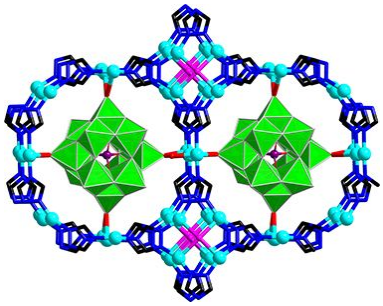	3D	$[PW_{12}O_{40}]^{3-}$	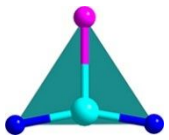 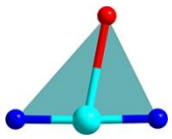 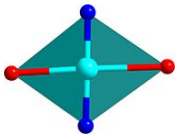 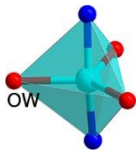	95	742

[a]Reaction conditions: 0.25 mmol of TMP, 1.25 μmol of catalyst 1.0 mL MeCN/H_2O (90:10, *V*/*V*), T = 80 °C, and 1.0 mmol of 30% H_2O_2. [b]Reaction conditions (reference S10): 0.25 mmol of TMP, 2.5 μmol of catalyst, 0.5 mL MeCN/H_2O (50:50, *V*/*V*), T = 80 °C, and 1.0 mmol of 30% H_2O_2. Color code: W, green; P, violet; Cu, light blue; O, red; N, blue; C, black; Cl, pink. OW: water molecule oxygen; OH: hydroxyl oxygen.

Table S3. Crystal Data and Structure Refinement for 1–4.

Complex	**1**	**2**	**3**	**4**
CCDC	2052779	2052780	2052781	2052782
Formula	$C_{36}H_{35}N_{30}PCu_6Mo_{12}O_{44}$	$C_{36}H_{39}N_{30}PCu_6W_{12}O_{46}$	$C_{24}H_{30}N_{20}PCu_3Mo_{12}O_{47}$	$C_{24}H_{33}N_{20}PCu_3W_{12}O_{48}$
Formula weight	3155.43	4246.38	2723.55	3797.49
T (K)	150(2)	150(2)	300(2)	300(2)
Crystal system	Triclinic	Triclinic	Triclinic	Monoclinic
Space group	*P-1*	*P-1*	*P-1*	*C*2/*c*
a (Å)	11.9921(9)	12.0101(11)	12.6464(6)	22.637(2)
b (Å)	12.3662(10)	12.3947(12)	12.6737(5)	13.9114(14)
c (Å)	13.9160(11)	13.9307(13)	23.6803(10)	20.363(3)
α (˚)	100.178(2)	99.945(3)	83.4100(10)	90
β (˚)	98.500(2)	98.598(3)	84.6350(10)	98.915(4)
γ (˚)	113.1483(17)	113.109(3)	61.3330(10)	90
V (Å^3)	1813.1(2)	1823.9(3)	3304.9(2)	6335.1(12)
Z	1	1	2	4
μ (mm^{-1})	3.858	20.682	3.278	22.819
Index ranges	-14 ≤ h ≤ 13 -14 ≤ k ≤ 14 -16 ≤ l ≤ 16	-14 ≤ h ≤ 14 -14 ≤ k ≤ 14 -16 ≤ l ≤ 16	-15 ≤ h ≤ 15 -15 ≤ k ≤ 15 -28 ≤ l ≤ 28	-26 ≤ h ≤ 25 -16 ≤ k ≤ 16 -23 ≤ l ≤ 24
Reflections collected	16652	22881	55319	22285
Independent reflections	6108	6428	11589	5572
R_{int}	0.0459	0.0456	0.0285	0.0339
Data/restraints/parameters	6108/84/629	6428/102/657	11589/108/1058	5572/90/545
GOF on F^2	1.027	1.048	1.208	1.213
R_1, wR_2 [$I > 2\sigma(I)$]	0.0443, 0.0918	0.0439, 0.1061	0.0488, 0.1045	0.0447, 0.0936
R_1, wR_2 (all data)	0.0710, 0.1037	0.0560, 0.1124	0.0509, 0.1053	0.0489, 0.0953

$R_1 = \Sigma||F_o| - |F_c||/\Sigma|F_o|$. $wR_2 = \Sigma[w(F_o^2 - F_c2)^2]/\Sigma[w(F_o^2)^2]^{1/2}$

Table S4. Selected Bond Lengths (Å) for POMCP 1.

bond	lengths (Å)	bond	lengths (Å)	bond	lengths (Å)
P(1)-O(18)	1.452(10)	Mo(3)-O(11)	1.653(6)	Mo(5)-O(17)	2.431(9)
P(1)-O(18)$^{\#1}$	1.452(10)	Mo(3)-O(5)	1.886(7)	Mo(6)-O(16)	1.658(5)
P(1)-O(19)	1.512(10)	Mo(3)-O(12)	1.904(7)	Mo(6)-O(14)	1.769(11)
P(1)-O(19)$^{\#1}$	1.512(10)	Mo(3)-O(10)	1.914(6)	Mo(6)-O(21)$^{\#1}$	1.864(12)
P(1)-O(20)$^{\#1}$	1.535(9)	Mo(3)-O(7)	1.947(6)	Mo(6)-O(3)	1.925(6)
P(1)-O(20)	1.535(9)	Mo(3)-O(20)	2.391(9)	Mo(6)-O(8)$^{\#1}$	1.934(7)
P(1)-O(17)	1.643(9)	Mo(3)-O(18)	2.477(9)	Mo(6)-O(21A)$^{\#1}$	2.002(11)
P(1)-O(17)$^{\#1}$	1.643(9)	Mo(4)-O(13)	1.653(6)	Mo(6)-O(14A)	2.046(13)
Mo(1)-O(1)	1.652(6)	Mo(4)-O(22)$^{\#1}$	1.853(11)	Mo(6)-O(17)$^{\#1}$	2.427(10)
Mo(1)-O(3)	1.887(6)	Mo(4)-O(6)	1.864(6)	Cu(1)-N(9)	1.958(6)
Mo(1)-O(2)	1.891(6)	Mo(4)-O(14)	1.882(11)	Cu(1)-N(2)	1.961(6)
Mo(1)-O(5)	1.928(7)	Mo(4)-O(10)	1.887(6)	Cu(1)-N(13)	2.095(7)
Mo(1)-O(4)	1.941(6)	Mo(4)-O(22A)$^{\#1}$	2.025(11)	Cu(2)-N(8)	1.922(7)
Mo(1)-O(20)	2.479(11)	Mo(4)-O(14A)	2.038(13)	Cu(2)-N(5)$^{\#2}$	1.950(6)
Mo(1)-O(19)$^{\#1}$	2.484(10)	Mo(4)-O(17)$^{\#1}$	2.366(9)	Cu(2)-N(12)	1.979(6)
Mo(2)-O(9)	1.653(6)	Mo(5)-O(15)	1.665(5)	Cu(3)-N(4)$^{\#3}$	1.953(6)
Mo(2)-O(7)	1.860(6)	Mo(5)-O(21)	1.826(13)	Cu(3)-N(14)	1.958(6)
Mo(2)-O(8)	1.898(6)	Mo(5)-O(22)	1.826(11)	Cu(3)-N(3)	2.040(6)
Mo(2)-O(6)	1.956(6)	Mo(5)-O(12)	1.877(8)	Cu(3)-O(16)	2.506(2)
Mo(2)-O(2)$^{\#1}$	1.985(6)	Mo(5)-O(4)	1.886(7)		
Mo(2)-O(19)	2.426(10)	Mo(5)-O(21A)	2.036(12)		
Mo(2)-O(18)	2.471(11)	Mo(5)-O(22A)	2.100(13)		

Symmetry transformations used to generate equivalent atoms: #1: -x+2, -y+2, -z; #2: x+1, y+1, z; #3: -x+2, -y+2, -z-1.

Table S5. Selected Bond Lengths (Å) for POMCP 2.

bond	lengths (Å)	bond	lengths (Å)	bond	lengths (Å)
P(1)-O(1)$^{\#1}$	1.438(17)	W(2)-O(13')	2.09(2)	W(5)-O(16)	1.921(10)
P(1)-O(1)	1.438(17)	W(2)-O(4)$^{\#1}$	2.428(15)	W(5)-O(14')	2.070(19)
P(1)-O(2)$^{\#1}$	1.509(16)	W(3)-O(12)	1.679(12)	W(5)-O(2)	2.443(16)
P(1)-O(2)	1.509(16)	W(3)-O(14)	1.858(17)	W(5)-O(3)	2.448(15)
P(1)-O(3)	1.515(15)	W(3)-O(13')	1.888(18)	W(6)-O(22)	1.660(9)
P(1)-O(3)$^{\#1}$	1.515(15)	W(3)-O(10)	1.894(10)	W(6)-O(7)	1.862(11)
P(1)-O(4)	1.659(15)	W(3)-O(11)	1.929(9)	W(6)-O(10)	1.863(10)
P(1)-O(4)$^{\#1}$	1.659(15)	W(3)-O(13)	1.946(17)	W(6)-O(19)	1.917(10)
W(1)-O(5)	1.663(9)	W(3)-O(14')	1.964(18)	W(6)-O(18)$^{\#1}$	1.925(11)
W(1)-O(9)	1.835(17)	W(3)-O(2)	2.387(16)	W(6)-O(3)$^{\#1}$	2.411(15)
W(1)-O(8)$^{\#1}$	1.877(16)	W(3)-O(1)	2.472(16)	W(6)-O(1)	2.473(16)
W(1)-O(7)$^{\#1}$	1.901(12)	W(4)-O(20)	1.674(10)	Cu(1)-N(12)	1.939(11)
W(1)-O(6)	1.928(11)	W(4)-O(9)	1.874(16)	Cu(1)-N(5)$^{\#2}$	1.950(10)
W(1)-O(8')$^{\#1}$	1.969(16)	W(4)-O(21)	1.898(17)	Cu(1)-N(7)	1.976(11)
W(1)-O(9')	2.080(17)	W(4)-O(19)	1.903(10)	Cu(2)-N(11)	1.952(11)
W(1)-O(4)	2.384(15)	W(4)-O(11)	1.918(10)	Cu(2)-N(2)	1.955(10)
W(2)-O(15)	1.664(8)	W(4)-O(21')	1.983(16)	Cu(2)-N(8)	2.097(10)
W(2)-O(13)	1.780(18)	W(4)-O(9')	2.032(17)	Cu(3)-N(4)$^{\#3}$	1.959(10)
W(2)-O(21)$^{\#1}$	1.819(17)	W(4)-O(4)	2.347(16)	Cu(3)-N(9)	1.960(10)
W(2)-O(8)	1.855(15)	W(5)-O(17)	1.677(10)	Cu(3)-N(3)	2.050(10)
W(2)-O(16)	1.923(11)	W(5)-O(14)	1.829(17)		
W(2)-O(8')	2.057(16)	W(5)-O(18)	1.891(11)		
W(2)-O(21')$^{\#1}$	2.089(17)	W(5)-O(6)	1.899(10)		

Symmetry transformations used to generate equivalent atoms: #1: -x-1, -y+2, -z-1; #2: x-1, y-1, z; #3: -x-1, -y+2, -z.

Table S6. Selected Bond Lengths (Å) for POMCP 3.

bond	lengths (Å)	bond	lengths (Å)	bond	lengths (Å)
P(1)-O(4)$^{\#1}$	1.459(10)	Mo(4)-O(21)	1.648(7)	Mo(9)-O(37)	1.962(7)
P(1)-O(4)	1.459(10)	Mo(4)-O(9)	1.725(13)	Mo(9)-O(36)	2.095(13)
P(1)-O(3)	1.464(10)	Mo(4)-O(5)	1.850(7)	Mo(9)-O(24)	2.439(9)
P(1)-O(3)$^{\#1}$	1.464(10)	Mo(4)-O(9A)	1.970(13)	Mo(9)-O(23)$^{\#2}$	2.453(9)
P(1)-O(1)$^{\#1}$	1.590(10)	Mo(4)-O(19)	1.979(8)	Mo(10)-O(38)	1.647(6)
P(1)-O(1)	1.590(10)	Mo(4)-O(11A)$^{\#1}$	2.014(13)	Mo(10)-O(27)	1.859(6)
P(1)-O(2)	1.620(10)	Mo(4)-O(11)$^{\#1}$	2.075(13)	Mo(10)-O(42)$^{\#2}$	1.889(7)
P(1)-O(2)$^{\#1}$	1.620(10)	Mo(4)-O(1)	2.393(11)	Mo(10)-O(28)	1.955(6)
P(2)-O(25)	1.490(9)	Mo(5)-O(7)	1.650(7)	Mo(10)-O(43)$^{\#2}$	1.967(7)
P(2)-O(25)$^{\#2}$	1.490(9)	Mo(5)-O(18)	1.813(8)	Mo(10)-O(23)	2.443(9)
P(2)-O(26)	1.528(9)	Mo(5)-O(8A)	1.824(12)	Mo(10)-O(25)	2.507(9)
P(2)-O(26)$^{\#2}$	1.528(9)	Mo(5)-O(8)	1.865(12)	Mo(11)-O(40)	1.647(6)
P(2)-O(23)$^{\#2}$	1.553(9)	Mo(5)-O(9)#1	1.917(13)	Mo(11)-O(28)	1.857(6)
P(2)-O(23)	1.553(9)	Mo(5)-O(17)$^{\#1}$	1.992(7)	Mo(11)-O(29)	1.898(6)
P(2)-O(24)$^{\#2}$	1.555(9)	Mo(5)-O(9A)$^{\#1}$	2.141(13)	Mo(11)-O(33)	1.962(6)
P(2)-O(24)	1.555(9)	Mo(5)-O(1)$^{\#1}$	2.392(10)	Mo(11)-O(34)	1.976(7)
Mo(1)-O(10)	1.656(8)	Mo(6)-O(12)	1.646(7)	Mo(11)-O(26)	2.406(9)
Mo(1)-O(14)	1.744(13)	Mo(6)-O(22)	1.844(7)	Mo(11)-O(25)	2.447(9)
Mo(1)-O(17)	1.815(7)	Mo(6)-O(19)	1.872(7)	Mo(12)-O(44)	1.648(6)
Mo(1)-O(14A)	1.953(14)	Mo(6)-O(18)	1.981(7)	Mo(12)-O(33)	1.858(7)
Mo(1)-O(22)$^{\#1}$	1.980(8)	Mo(6)-O(20)	2.012(8)	Mo(12)-O(37)	1.896(7)
Mo(1)-O(13A)	2.016(13)	Mo(6)-O(3)	2.421(10)	Mo(12)-O(27)	1.965(6)
Mo(1)-O(13)	2.059(13)	Mo(6)-O(4)	2.419(10)	Mo(12)-O(41)	1.987(7)
Mo(1)-O(2)	2.369(10)	Mo(7)-O(39)	1.644(6)	Mo(12)-O(24)	2.460(9)
Mo(2)-O(6)	1.653(8)	Mo(7)-O(36A)	1.792(12)	Mo(12)-O(25)	2.516(9)
Mo(2)-O(20)	1.798(9)	Mo(7)-O(34)	1.828(7)	Cu(1)-N(2)	1.994(6)
Mo(2)-O(15)	1.848(13)	Mo(7)-O(36)	1.903(13)	Cu(1)-N(7)	2.021(6)
Mo(2)-O(15A)	1.872(13)	Mo(7)-O(42)	1.978(7)	Cu(1)-O(1H)	2.036(5)

Mo(2)-O(14)	1.906(12)	Mo(7)-O(32)$^{\#2}$	1.982(7)	Cu(1)-N(15)$^{\#3}$	2.037(6)
Mo(2)-O(5)	2.002(7)	Mo(7)-O(23)$^{\#2}$	2.476(10)	Cu(1)-O(1W)	2.248(7)
Mo(2)-O(14A)	2.177(16)	Mo(7)-O(26)	2.499(10)	Cu(1)-O30	2.614(4)
Mo(2)-O(2)	2.404(10)	Mo(8)-O(31)	1.653(6)	Cu(2)-N(3)	1.971(6)
Mo(3)-O(11)	1.650(12)	Mo(8)-O(41)	1.844(7)	Cu(2)-N(10)$^{\#4}$	1.981(6)
Mo(3)-O(13)	1.651(13)	Mo(8)-O(32)	1.888(7)	Cu(2)-N(13)	2.030(6)
Mo(3)-O(16)	1.686(6)	Mo(8)-O(29)$^{\#2}$	1.967(7)	Cu(2)-O(1H)	2.031(4)
Mo(3)-O(8)	1.883(12)	Mo(8)-O(35)	1.968(7)	Cu(2)-N(17)	2.303(6)
Mo(3)-O(15)	1.916(13)	Mo(8)-O(24)	2.470(10)	Cu(3)-N(5)$^{\#5}$	2.001(6)
Mo(3)-O(11A)	2.0316(15)	Mo(8)-O(26)$^{\#2}$	2.513(9)	Cu(3)-N(8)	2.021(6)
Mo(3)-O(13A)	2.045(15)	Mo(9)-O(30)	1.643(5)	Cu(3)-N(12)	2.036(6)
Mo(3)-O(15A)	2.180(14)	Mo(9)-O(35)	1.851(7)	Cu(3)-O(1H)	2.044(5)
Mo(3)-O(8A)	2.179(12)	Mo(9)-O(43)	1.884(7)	Cu(3)-N(16)	2.361(6)
Mo(3)-O(2)	2.512(10)	Mo(9)-O(36A)	1.906(12)	Cu(3)-O(16)	2.727(7)

Symmetry transformations used to generate equivalent atoms: #1: -x-2, -y+3, -z+1; #2: -x, -y+2, -z; #3: x+1, y-1, z; #4: x, y+1, z; #5: x-1, y, z.

Table S7. Selected Bond Lengths (Å) for POMCP 4.

bond	lengths(Å)	bond	lengths(Å)	bond	lengths(Å)
P(1)-O(3)$^{\#1}$	1.429(15)	W(3)-O(6A)	1.916(19)	W(6)-O(1)	2.451(16)
P(1)-O(3)	1.429(15)	W(3)-O(6)	1.957(17)	W(6)-O(1)$^{\#1}$	2.451(16)
P(1)-O(4)$^{\#1}$	1.530(15)	W(3)-O(7)	2.032(17)	W(7)-O(8)	1.640(9)
P(1)-O(4)	1.530(15)	W(3)-O(2)	2.396(14)	W(7)-O(6)	1.890(18)
P(1)-O(1)	1.536(16)	W(4)-O(20)	1.651(14)	W(7)-O(22)	1.901(19)
P(1)-O(1)$^{\#1}$	1.536(16)	W(4)-O(13)	1.884(11)	W(7)-O(5)	1.926(16)
P(1)-O(2)	1.647(14)	W(4)-O(13)$^{\#1}$	1.884(11)	W(7)-O(16)	2.082(15)
P(1)-O(2)$^{\#1}$	1.647(14)	W(4)-O(19)	1.891(10)	W(7)-O(2)	2.427(15)
W(1)-O(9)	1.685(9)	W(4)-O(19)$^{\#1}$	1.891(10)	W(7A)-O(16)	1.662(14)
W(1)-O(13)	1.910(11)	W(4)-O(4)	2.480(15)	W(7A)-O(8)	1.802(9)
W(1)-O(12)	1.914(9)	W(4)-O(4)$^{\#1}$	2.480(15)	W(7A)-O(5A)	1.891(16)
W(1)-O(10)$^{\#1}$	1.919(9)	W(5)-O(21)	1.662(11)	W(7A)-O(22A)	1.912(18)
W(1)-O(11)#1	1.920(10)	W(5)-O(7A)	1.866(17)	W(7A)-O(6A)	1.938(18)
W(1)-O(4)	2.372(15)	W(5)-O(10)	1.892(10)	W(7A)-O(1)	2.422(17)
W(1)-O(3)	2.475(16)	W(5)-O(14)	1.900(11)	W(7A)-O(2)	2.509(15)
W(2)-O(15)	1.657(11)	W(5)-O(5A)	1.936(16)	Cu(1)-N(10)$^{\#2}$	1.997(10)
W(2)-O(14)	1.918(9)	W(5)-O(5)	1.959(16)	Cu(1)-N(3)	2.002(11)
W(2)-O(11)	1.921(9)	W(5)-O(7)	2.061(17)	Cu(1)-O(2W)	2.012(9)
W(2)-O(17)$^{\#1}$	1.938(11)	W(5)-O(2)	2.356(14)	Cu(1)-N(8)	2.012(10)
W(2)-O(16)$^{\#1}$	1.946(12)	W(6)-O(23)	1.662(17)	Cu(1)-O(8)	2.423(9)
W(2)-O(1)$^{\#1}$	2.370(16)	W(6)-O(22A)$^{\#1}$	1.777(16)	Cu(1)-O1W	2.509(2)
W(2)-O(3)$^{\#1}$	2.492(14)	W(6)-O(22A)	1.777(16)	Cu(2)-N(7)$^{\#3}$	1.977(10)
W(3)-O(18)	1.676(10)	W(6)-O(17)$^{\#1}$	1.889(12)	Cu(2)-N(2)$^{\#3}$	2.003(10)
W(3)-O(7A)	1.830(18)	W(6)-O(17)	1.889(12)	Cu(2)-N(2)	2.003(10)
W(3)-O(19)	1.885(10)	W(6)-O(22)	2.07(2)	Cu(2)-O(1W)$^{\#3}$	2.385(10)
W(3)-O(12)	1.900(11)	W(6)-O(22)$^{\#1}$	2.07(2)	Cu(2)-O(1W)	2.385(10)

Symmetry transformations used to generate equivalent atoms: #1: -x+1, y, -z-1/2; #2: x, -y+1, z-1/2; #3: -x+3/2, -y+1/2, -z.

V. References

(S1)John, C. B. J., Phosphotungstic Acid. In *Inorg. Synth.*, Booth, H. S., Ed. John Wiley & Sons.: 1939; Vol. 1, pp 132−133.

(S2)DOMAILLE, P. J., Vanadium(V) Substituted Dodecatungstophosphates. In *Inorg. Synth.*, Ginsberg, A. P., Ed. John Wiley & Sons.: 1990; Vol. 27, pp 96−104.

(S3)Brevard, C.; Schimpf, R.; Tourne, G.; Tourne, C. M., ^{183}W NMR: A Complete and Unequivocal Assignment of the W-W Connectivities in Heteropolytungstates via Two-Dimensional ^{183}W NMR Techniques. *J. Am. Chem. Soc.* **1983,** *105*, 7059−7063.

(S4)Wu, H., Contribution to the Chemistry of Phosphomolybdic Acids, Phosphotungstic Acids, and Allied Substances. *J. Biol. Chem.* **1920,** *43*, 189−220.

(S5)Filowitz, M.; Ho, R. K. C.; Klemperer, W. G.; Shum, W., Oxygen-17 Nuclear Magnetic Resonance Spectroscopy of Polyoxometalates. 1. Sensitivity and Resolution. *Inorg. Chem.* **1979,** *18*, 93−103.

(S6)Detert, H., (E)-1,2-Bis(5-aryl-1,3,4-oxadiazol-2-yl)ethenes. *Synthesis* **1999,** *1999*, 999−1004.

(S7)Ouellette, W.; Zubieta, J., Solid State Coordination Chemistry of Microporous Metal-Organic Frameworks of the Cadmium(II)-4-Pyridyltetrazolate Family: the Structural Influences of Chloride Incorporation. *Chem. Commun.* **2009**, 4533−4535.

(S8)Sheldrick, G. M., *SHELXS97 and SHELXL97. Program for Crystal Structure Solution and Refinement*. University of Göttingen: Göttingen, Germany, 1997.

(S9)Sheldrick, G. M., SHELXT-Integrated Space-Group and Crystal-Structure Determination. *Acta Crystallogr., Sect. A: Found. Adv.* **2015,** *71*, 3−8.

(S10) Chang, S. Z.; An, H. Y.; Chen, Y. H.; Hou, Y. J.; Zhang, J.; Zhu, Q. S., Multiunit Catalysts with Synergistic Reactivity: Three-Dimensional Polyoxometalate-Based Coordination Polymers for Highly Efficient Synthesis of Functionalized *p*-Benzoquinones. *ACS Appl. Mater. Interfaces* **2019,** *11*, 37908−37919.